62p. 001

UNIVERSITY OF NEW MEXICO

ALBUQUERQUE

ENGINEERING EXPERIMENT STATION

SEMI-ANNUAL STATUS REPORT
A STUDY OF THE HALL EFFECT AND MAGNETORESISTANCE FOR LOW VOLTAGE, HIGH CURRENT, DC TO AC CONVERSION

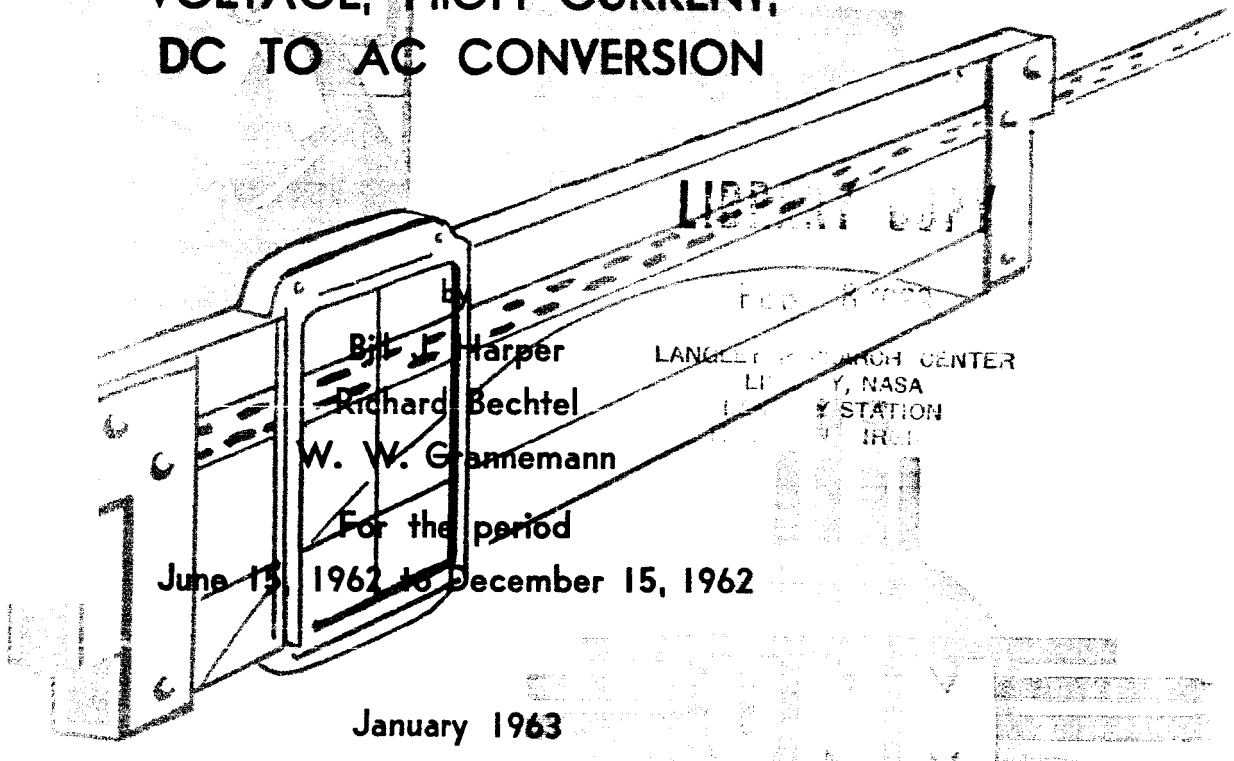

By
Bill J. Harper
Richard Bechtel
W. W. Grannemann

For the period
June 15, 1962 to December 15, 1962

January 1963

National Aeronautics and
Space Administration
Grant NsG 279-62

SEMI-ANNUAL STATUS REPORT

A STUDY OF THE HALL EFFECT AND MAGNETORESISTANCE FOR LOW VOLTAGE, HIGH CURRENT, DC TO AC CONVERSION

by

Bill J. Harper
Richard Bechtel
W. W. Grannemann

For the period
June 15, 1962 to December 15, 1962

National Aeronautics and
Space Administration
Grant NsG 279-62

January 1963

TABLE OF CONTENTS

LIST OF FIGURES

CHAPTER I. INTRODUCTION

This status report presents a discussion of the applicability of the Hall effect and magnetoresistance as a controlled rectifier in a low voltage, high current d.c. to a.c. converter. A controlled rectifier using magnetoresistance has a very low impedance with no control field applied. This impedance can be made considerably lower than the best existing transistors when operated at low voltages. The major problem with the magnetoresistance controlled rectifier is in obtaining a high on-field resistance as compared to the power transistor where there is difficulty in obtaining a low saturation resistance at low voltages.

The magnetoresistance controlled rectifier efficiency is relatively independent of source voltage when used in a converter, while the transistor efficiency is highly dependent on source voltage.

The first phase of this research was on the study of the general theory of magnetoresistance as it applied to semiconductor devices used as controlled rectifiers. The associated experimental study on magnetoresistance devices used indium antimonide as the semiconductor material.

Magnetoresistance is a function of the material, the configuration of the semiconductor material and compound, and the temperature. Most of the theoretical and experimental

effort has been devoted to the rectangular slab configuration and the corbino disk configuration.

Two circuit configurations have been analyzed using the magnetoresistance elements as a controlled rectifier and computing the efficiency with on-field to off-field ratios of the magnetoresistance device. Neglecting circuit losses and using an on-field to off-field resistance ratio of 50, the theoretical efficiency is about 57%.

CHAPTER II THEORY OF MAGNETORESISTIVE DEVICES

General Theory of Magnetoresistance

1.0 The Phenomenological Equation

If a current carrying conductor (or semiconductor) is placed in a magnetic field $\bar{H}$, the Lorentz force on a charge carrier with charge q and effective mass m is:[1]

$$\bar{F} = \frac{d\bar{P}}{dt} = q\,\bar{E} + q/c(\bar{v} \times \bar{H}) \qquad (2\text{-}1)$$

where: $\bar{P} = m\bar{v}$ = charge carrier momentum
$\bar{v}$ = charge carrier velocity
$\bar{E}$ = electric field
$\bar{H}$ = magnetic field
c = velocity of light.

For a material in which the momentum of the charge carrier is governed by a finite mean free time between collisions τ, the equation (2-1) becomes:

$$\frac{d\bar{P}}{dt} = \frac{\bar{P}}{\tau} = q\,\bar{E} + q/c(\bar{v} \times \bar{H}), \qquad (2\text{-}2)$$

With the assumption that the charge carrier occupies an energy level near the top of the valence band, then $\bar{P} = m\bar{v}$ and:

$$\bar{v} = \frac{q\tau}{m}\,\bar{E} + \frac{q\tau}{mc}(\bar{v} \times \bar{H}). \qquad (2\text{-}3)$$

A density ρ of positive charge carriers moving with velocity $\bar{v}$ results in a current density:

$$\bar{J}_p = \rho q\bar{v} = \rho q(\frac{q\tau}{m})\,\bar{E} + \frac{\rho}{c}(\frac{q\tau}{m})(\bar{J}_p \times \bar{H}) \qquad (2\text{-}4)$$

---

[1] Shockley, William, Electrons and Holes in Semiconductors, D. Van Norstrand Company, Inc., New York, p 180, 1950.

which can be rewritten as:

$$\bar{J}_p = \sigma_p \bar{E} + \mu_p/c \; (\bar{J}_p \times \bar{H}) \qquad (2\text{-}5)$$

where: $\sigma_p = q\rho\mu_p$ = conductivity of material

μ_p = charge carrier mobility.

The equation (2-5) is referred to as the phenomenological equation describing the galvanomagnetic properties of a positive carrier type conductor under the influence of magnetic and electric fields.

For materials in which electrons are the only charge carrier, the equation describing the relationship between current density, electric field and magnetic field becomes:

$$\bar{J}_n = \sigma_n \bar{E} - \mu_n/c \; (\bar{J}_n \times \bar{H}) \qquad (2\text{-}6)$$

where the various parameters are defined for electrons rather than holes as in equation (2-5).

If both types of carriers are significant, the phenomenological equation becomes:

$$\bar{J} = \sigma \bar{E} + \frac{1}{c}(\mu_p \bar{J}_p - \mu_n \bar{J}_n) \times \bar{H} \qquad (2\text{-}7)$$

where: $\sigma = \sigma_p + \sigma_n = |e|(\mu_p \rho + \mu_n N)$

$\bar{J} = \bar{J}_n + \bar{J}_p$.

For the remainder of this report, the equation (2-6) for n type indium antimonide will be of primary interest.

2.0 The Hall Effect

The solution of equation (2.6) for the electric field $\bar{E}$ yields the result:

$$\bar{E} = \frac{1}{\sigma_n} \bar{J}_n + \frac{\mu_n}{\sigma_n c} (\bar{J}_n \times \bar{H}). \qquad (2\text{-}8)$$

This equation indicates that in a material such as InSb with a component of magnetic field transverse to the current density, the electric field contains a component which is normal to both $\bar{J}_n$ and $\bar{H}$. This component of electric field is called the Hall field, and the coefficient:

$$R_H = - \frac{\mu_n}{\sigma_n c} = - \frac{1}{nec} \qquad (2\text{-}9)$$

is defined as the Hall constant of the n type material. In general, for materials other than simple metals and degenerate semiconductors, the expression for the Hall constant may be quite a complicated function of energy distributions, scattering potentials and similar properties of the material. This complication results from the fact that in general, the assumption of mean free time being independent of the charge carrier energy (implied in equation 2-2) is not a valid representation. Thus, for those materials in which the approximation:

$$\frac{d\bar{P}}{dt} = \frac{\bar{P}}{\tau} \qquad (2\text{-}10)$$

is not valid, the mean free time between collisions is a function of the electron energy and the dominant scattering mechanism within the crystal. In the derivation of the equations which describe the mechanism whereby the magnetoresistive effect occurs, one approach is to consider the effect of deviation of the constant energy surfaces from the simple spherical shape.[1]

---

[1] Ibid, pp. 336-341

Another approach which has proved to be useful is to consider the quantization of the charge carrier energies due to the strong magnetic field.[1]

3.0 The Classical Magnetoresistance Effect

The application of a magnetic field to a current carrying conductor usually alters the resistivity of the conductor. The more common effect of the magnetic field is to increase the resistivity of the conductor although some cases of negative magnetoresistance have been observed. For normal magnetoresistance, it has been shown that the variation of resistivity due to a magnetic field obeys Kohler's rule:[2]

$$\frac{\rho(H) - \rho_o}{\rho_o} = F\left(\frac{H}{\rho_o}\right) \qquad (2\text{-}11)$$

where: ρ_o = zero field resistivity

$\rho(H)$= resistivity with applied field H,

and F is a function depending only on the physical properties and geometrical configuration of the conductor being observed.

The equation (2-6) can be modified to a more suitable form in the following manner:

$$\bar{J} = \sigma \bar{E} - \mu/c \, (\bar{J} \times \bar{H}). \qquad (2\text{-}6)$$

Substitute (2-6) into the right hand side of the equation for $\bar{J}$ and solve for $\bar{J}$.

---

[1] Adams, E. N. and Holstein, T. D.,"Quantum Theory of Transverse Galvanomagnetic Phenomena", J. Phys. Chem. Solids, Vol. 10, pp. 254-276, 1959.

[2] Ziman, J. M., Electrons and Phonons, Oxford Press, London, 1960, p.491.

$$\bar{J} = \sigma\bar{E} - \mu/c \left\{ \left[\bar{E} - /c(\bar{J} \times \bar{H})\right] \times \bar{H} \right\}$$

$$\bar{J} = \sigma\bar{E} - \mu\sigma/c\ (\bar{E} \times \bar{H}) + \mu^2/c^2 \left[(\bar{J} \times \bar{H}) \times \bar{H}\right]$$

$$\bar{J} = \sigma\bar{E} - \mu\sigma/c\ (\bar{E} \times \bar{H}) - \mu^2H^2/c^2\bar{J} \qquad (2\text{-}12)$$

$$\bar{J}(1 + \mu^2H^2/c^2) = \sigma\bar{E} - \mu\sigma/c(\bar{E} \times \bar{H})$$

$$\bar{J} = \left[\sigma/(1 + \mu^2H^2/c^2)\right]\bar{E} - \left[(\mu/c)\,\sigma/(1 + \mu^2H^2/c^2)\right](\bar{E}\times\bar{H}).$$

From this equation, it is seen that for transverse $\bar{E}$ and $\bar{H}$ fields applied to a conductor with normal conductivity σ, the resultant current density in the conductor consists of a component parallel to the applied field and a component normal to the applied field. These components of current density can be interpreted as resulting from the product of a magnetic field dependent conductivity with the applied electric field, and the second component consists of the product of the same magnetic field dependent conductivity with a magnetic dependent electric field normal to the applied electric field. With this interpretation, equation (2-12) becomes:

$$\bar{J} = \sigma_H\,\bar{E} - \sigma_H\,\bar{E}_H \quad ; \qquad (2\text{-}13)$$

where:

$\bar{J}$ = net current density,

$\sigma_H = \sigma/(1 + \mu^2H^2/c^2)$, effective conductivity,

$\bar{E}$ = applied electric field,

$E_H = (\mu H/c)|\bar{E}|$, resultant electric field normal to $\bar{E}$.

On the basis of this equation, the resistivity of the material would vary quadratically with the applied magnetic field H,

$$\rho_H = \frac{1}{\sigma_H} = \frac{1}{\sigma} \cdot \frac{1}{1 + \mu^2H^2/c^2} \qquad (2\text{-}14)$$

As pointed out previously, the derivation of the magnetoresistance effect by this classical method is appropriate only for simple metals and degenerate semiconductors in which the energy surface are spherical, and the relaxation time is independent of energy. The classical derivation always has as its result, a quadratic dependence of the resistivity on the magnetic field H. There are many intermetalic and semiconductor compounds which experimentally do not behave in this manner. In order to explain the galvanomagnetic phenomena peculiar to these materials, more elaborate methods of analysis must be employed

4.0 The Magnetoresistance Effect in InSb

Rather than the classical quadratic dependence of magnetoresistance on magnetic field, the compound semiconductor InSb displays a change in resistivity which is proportional to the magnetic field. The explanation of this deviation from the classical results has been investigated theoretically by a number of authors for restricted ranges of temperature and magnetic field. In particular, it has been shown that in a strong magnetic field, electron motion normal to the field becomes quantized such that the density of electron energy levels and the scattering matrices become functions of the magnetic field.[1] These results have been applied to the investigation of magnetoresistance in InSb.[2] Several different

---

[1] Adams and Holstein, op. cit.

[2] Sladek, R. J., "Magnetoresistance of High Purity InSb in the Quantum Limit," J. Phys. Chem. Solids, Vol. 16, 1960, pp 1-9.

scattering models have been assumed by the various authors, but the net conclusion in each case is that for high purity n-type InSb, the magnetoresistance is a linear function of H for values of H above a few hundred gauss. In weak fields, it has been shown that the magnetoresistance varies from a H^2 dependence to a linear dependence as the field is increased from 0 to a few hundred gauss.[1]

In those applications where fields of 10 Kilogauss or more are utilized, the magnetoresistance of InSb is essentially a linear function of H. That is, the resistivity of InSb can be expressed as

$$\rho_H = \rho_o (1 + KH) \quad ; \qquad (2\text{-}15)$$

where ρ_H = resistivity in magnetic field H,

ρ_o = zero field resistivity,

K = proportionality constant.

In general, the proportionality constant K is primarily a function of the mobility and the temperature. It is independent of the geometry of the InSb sample. The net magnetoresistance of an InSb sample is a function of its geometry.

5.0 Magnetoresistive Devices

5.1 The Rectangular Slab

Consider a rectangular slab of InSb, shown in Figure 2-1, which has a zero field resistivity σ_o.

---

[1] Bate, R. T., Willardson, R. K., and Beer, A. C., "Transverse Magnetoresistance and Hall Effect in N-Type InSb," J. Phys. Chem. Solids, Vol. 9, 1959, pp 119-128.

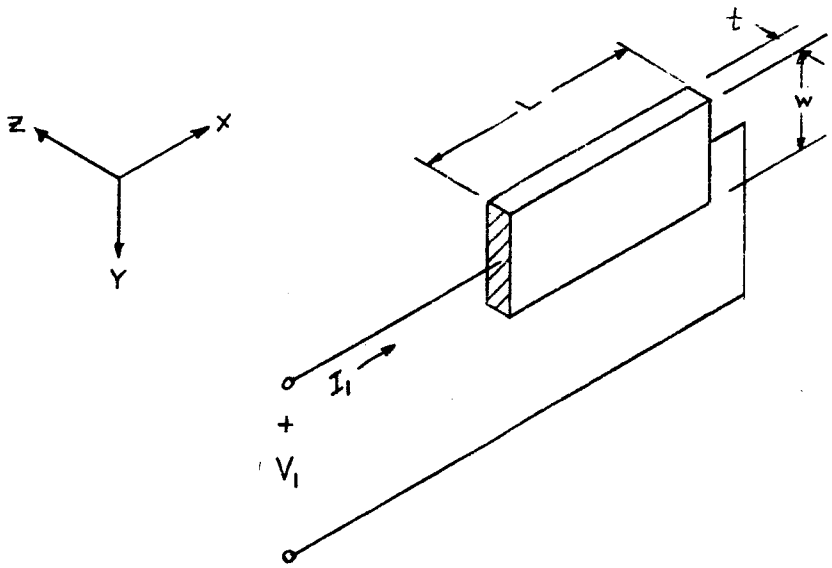

Figure 2-1 - InSb Rectangular Slab

The zero field resistance of the slab is:

$$R_o = \rho_o L/wt \quad , \tag{2-16}$$

It would appear that with a magnetic field H applied in the z direction, the resistance, R, of the slab would vary with H as

$$R = \rho_o L/wt(1 + KH) \quad . \tag{2-17}$$

This is not the case, however, since a Hall field in the y direction results from the cross product of the current density and the magnetic field. The effect of this Hall field is to reduce the actual magnetoresistance of the slab below that predicted by equation (2-17) above, such that:

$$R = R_o(1 + K_1H) - K_2H \quad ; \tag{2-18}$$

where: $R_o = \rho_o L/wt$, zero field resistance,

K_1 = proportionality constant for bulk InSb,

K_2 = proportionality constant due to geometry.

The exact dependence of K_2 upon the geometry and the physical properties of InSb is not available at the present time. Sufficient experimental data to determine the geometrical dependence of K_2 will be obtained in the near future. It has been found, however, that the value of K_2 can be sufficiently large to decrease the magnetoresistance of the rectangular slab to 1/3 that of the bulk material.

From the above discussion, it is evident that in order to maximize the magnetoresistance of an InSb sample, the effect of the resultant Hall field on the magnetoresistance must be minimized. It has been found experimentally, for the rectangular slab, that the magnetoresistance could be increased by several percent if the lengthwise edges of the slab were electrically connected as shown in Figure 2-2.

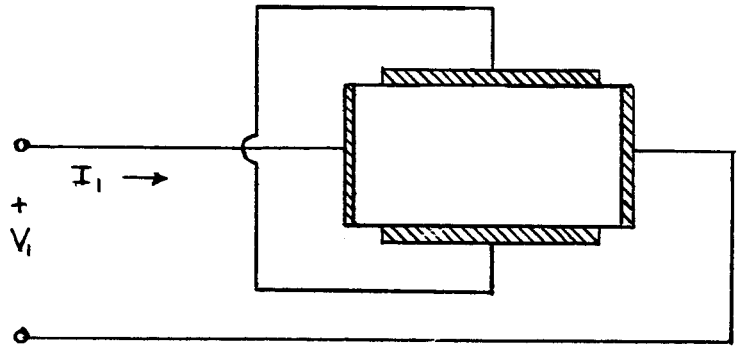

Figure 2-2 Modified Rectangular Slab

This modification of the slab results in a minimum Hall field being developed across the device, which in turn appears to reduce the value of K_2 in equation (2-18). A more detailed discussion of the magnetoresistance of the modified rectangular slab is contained in Chapter III.

6.0 The Corbino Disk

A geometrical configuration which has certain advantages over the rectangular slab is shown in Figure 2-3. This configuration is called a Corbino Disk after O. M. Corbino who in 1911 reported magnetoresistance measurements on several metals in which the samples were disks with inner and outer concentric ring contacts.[1]

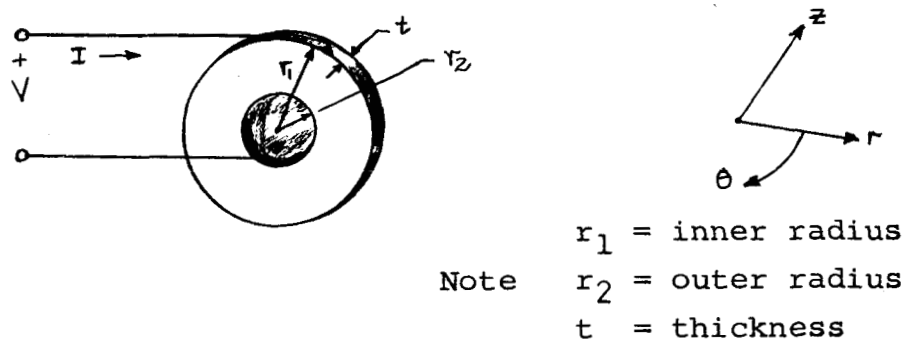

Note r_1 = inner radius
r_2 = outer radius
t = thickness

Figure 2-3 Corbino Disk

In the absence of a magnetic field, the current flow is radial, and the zero-field resistance of the disk is:

$$R_o = \frac{\rho_o}{2\pi t} \log_e \frac{r_2}{r_1} \quad ; \qquad (2\text{-}19)$$

where ρ_o is the zero-field resistivity.

With a magnetic field applied parallel to the axis of the disk, the current desnity will then have a component in the θ direction in addition to its radial component. Because of the geometrical symmetry, no Hall field can exist in the θ direction due to the radial component of current density. The only Hall field which can exist within the disk is parallel to its axis. This Hall field in the z direction results from the θ component of current density. Since the θ component of current density

[1] Corbino, O. M., Atti. Acad. Nazl., Lincei 20, 1911.

is proportional to the radial component, and the Hall field in the z direction is proportional to the θ component, the Hall field is proportional to the input current as in the case of the rectangular slab. In this situation, however, the proportionality constant relating the Hall field and the input current is small in comparison with that found in the rectangular slab. The resistance of the disk can be expressed as:

$$R = R_o(1 + K_1 H) - K_2 F(H) \quad ; \qquad (2\text{-}20)$$

where R_o = zero field resistance,

K_1 = proportionality constant of bulk InSb,

K_2 = proportionality constant due to geometry,

and $F(H)$ is a function of the magnetic field. The equation (2-20) has the same form as (2-18) except that here, the subtractive factor is much less than that contained in (2-18). Also, the exact form $F(H)$ takes is questionable. The theory of the disk presented above would indicate that $F(H)$ is of the form:

$$F(H) = H + \lambda_1 H^2 \quad , \qquad (2\text{-}20)$$

The experimental data for various disks indicate no variation of resistance proportional to H^2 for fields above a few hundred gauss. Thus, it would appear that for field up to 22 Kilogauss, the coefficient λ_1 is so small that the H^2 term can be neglected.[1]

---

[1]This conclusion is valid only for high-purity n-type polycrystalline InSb. For example: Green, Milton, "Corbino Disk Magnetoresistivity Measurements on InSb," Journal of Applied Physics, Vol. 32, No. 7, 1961, lists results for single crystal InSb in which the magnetoresistance varies with H^2 for fields up to 4-6 Kilogauss, varies as H for fields of 6-15 Kilogauss and then begins to approach a zero slope for fields in the vicinity of 20 Kilogauss.

As in the case of the rectangular slab, more experimental data is needed before the exact dependence of the magnetoresistance upon the physical properties of InSb and the sample geometry can be determined.

7.0 Miscellaneous Configurations

In addition to the rectangular slab and the Corbino disk, various other geometrical configurations have been experimentally investigated. In general, these specimens have been the scraps obtained from cutting rectangular slabs and disks from InSb ingots. Suprisingly enough, some of these rather odd-shaped pieces have exhibited magnetoresistance characteristics on a par with the better modified rectangular slabs and Corbino disks. These unexpected high magnetoresistances are attributed to the fact that in each case where this occurred, the geometry and contact arrangement were such that the Hall effect was minimized.

Again, the theoretical and experimental problems associated with these irregular shapes consist of determining the variation of magnetoresistance with sample geometry and the properties of InSb.

8.0 The Symmetrical Four-Terminal Magnetoresistor

An interesting extension of the rectangular slab is shown in Figure 2-4. Here a square specimen with four symmetrical contacts is subjected to a transverse magnetic field H.

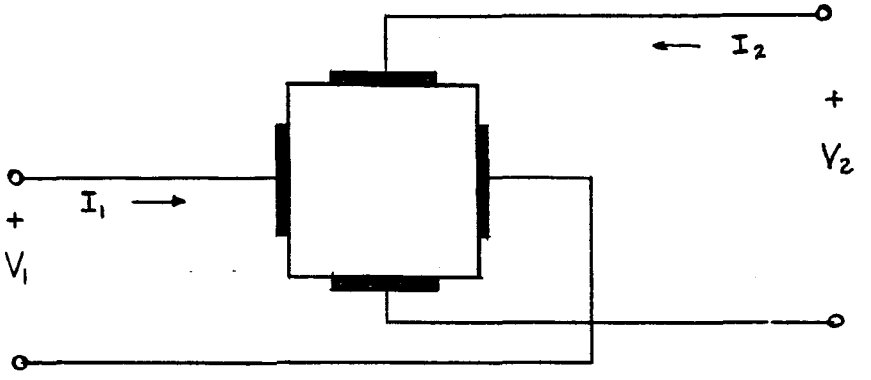

Figure 2-4 Duo Magnetoresistor

The four-terminal open-circuit impedance equations for this configuration are:

$$V_1 = I_1 R_{11} + I_2 R_{12} \quad ,$$
$$V_2 = I_1 R_{21} + I_2 R_{22} \quad . \qquad (2\text{-}21)$$

The R_{11} parameter is defined by:

$$R_{11} = V_1/I_1 \Big|_{I_2=0} \quad ;$$

which is simply equation (2-18) for the rectangular slab with the appropriate values of K_1 and K_2 inserted. Because of the symmetry, the parameters R_{22} and R_{11} are equal, and have the value:

$$R_{11} = R_{22} = R_o(1 + KH) \quad ; \qquad (2\text{-}22)$$

where $K = K_1 - K_2$.

The parameter R_{12} is defined by:

$$R_{12} = \frac{V_1}{I_2} \Big|_{I_1=0} \quad ; \qquad (2\text{-}23)$$

which is simply the ratio of the Hall voltage, due to the cross product of I_2 and H, to I_2. For the rectangular slab, the Hall voltage is:

$$V_1 = \pm \lambda H I_2 \quad , \qquad (2\text{-}24)$$

so that:

$$R_{12} = \pm \lambda H \quad ; \tag{2-25}$$

where λ is a constant of proportionality and the $\pm$ sign results from the direction dependence of the sign of the cross product $(\bar{I}_2 \times \bar{H})$. Again, because of the symmetry

$$R_{21} = - R_{21} = \mp \lambda H \quad , \tag{2-26}$$

where the negative value of R_{21} results from the direction dependence of the cross product $(\bar{I}_1 \times \bar{H})$.

With the values of the parameters determined above, the set of four-terminal equations become:

$$\begin{aligned} V_1 &= I_1 R_o(1 + KH) \pm \lambda H I_2 \quad , \\ V_2 &= I_2 R_o(1 + KH) \mp \lambda H I_1 \quad . \end{aligned} \tag{2-27}$$

If V_1 and V_2 represent identical low-impedance voltage sources, then:

$$V_1 = V_2 = V \quad ,$$

and: $$I_1 R_o(1 + KH) \pm \lambda H I_2 = I_2 R_o(1 + KH) \mp \lambda H I_1 \quad ,$$

which yields the ratio:

$$I_1/I_2 = \frac{R_o(1+KH) \mp \lambda H}{R_o(1+KH) \pm \lambda H} \quad . \tag{2-28}$$

This expression also represents the ratio R_2/R_1 where R_2 and R_1 are the input resistances:

$$R_2 = \frac{V_2}{I_2} = \frac{V}{I_2} \quad ,$$

$$R_1 = \frac{V_1}{I_1} = \frac{V}{I_1} \quad .$$

It is seen that when the magnetic field is in one direction, $R_2 > R_1$ and when the field is reversed, $R_1 > R_2$. Reversing the

magnetic field has the effect of interchanging the roles of R_1 and R_2. When R_1 has a maximum value, R_2 is a minimum; and R_2 has a maximum value when R_1 is a minimum.

The characteristics of the input resistance of one terminal pair can be varied considerably by adjusting the current in the second terminal pair. For example, in equation (2-27), the voltage V_1 can be made zero for a field H by selecting I_2 to have the value:

$$I_2 = I_1 \frac{R_o(1+KH)}{\lambda H} \quad . \tag{2-29}$$

Then:

$$V_1 = I_1 \left[R_o(1 + KH) \pm R_o(1 + KH) \right] \quad ,$$

and the input resistance becomes

$$R_1 = V_1/I_1 = 2R_o(1 + KH) \tag{2-30}$$

for H in one direction, and:

$$R_1 = V_1/I_1 = 0 \tag{2-31}$$

for H in the opposite direction.

The experimental results agree quite well with the theoretical behavior predicted by the equation (2-27). Several experimental curves for this configureation are contained in Chapter III.

9.0 Variation of Magnetoresistance With Temperature

As the temperature of a InSb specimen is decreased from room temperature ($300^{o}K$), the resistivity, mobility, and Hall constant increase by varying amounts.[1] Since the magneto-

---

[1] Green, Milton, Op. cit.

resistance exhibited by the specimen depends upon all three of these parameters, it is apparent that the magnetoresistance is also dependent upon the temperature.

A comprehensive theory of the variation of magnetoresistance with temperature is not available at the present time. It has been found experimentally, that the magnetoresistance of a specimen increases with decreasing temperature.[1] The greatest increase in magnetoresistance occurs at low and moderate values of magnetic fields. For high fields of 20 kilogauss or more, the magnetoresistance may exhibit very little change with decreasing temperature.

Conclusion

It has been shown that the classical theory of magnetoresistance as derived from the free electron model and the phenomenological equation is not applicable to high pruity InSb. The failure of the classical theory is attributed to the fact that in InSb, both the density of energy levels and the scattering mechanism are functions of the magnetic field. The magnetoresistance effects predicted by quantum theory vary from a quadratic dependence upon H for low fields, to a linear dependence upon H for high fields. For InSb specimens in which the transverse magnetic field is varied to a value of several kilogauss, the magnetoresistance is essentially a linear function of H.

The geometry of the sample has a large effect upon the magnetoresistance of the specimen. The maximum magnetoresistance

---

[1] Ibid.

occurs in a specimen in which the effect of the Hall field is minimized. Of the more common geometrical shapes, the Corbino disk exhibits the maximum magnetoresistance for a given InSb sample.

A comprehensive theoretical study of the dependence of the magnetoresistance upon sample geometry, physical properties and temperature will be continued in conjunction with similar experimental studies. The primary goal of these studies is to maximize the magnetoresistance for InSb specimens.

CHAPTER III. EXPERIMENTAL MAGNETORESISTANCE DEVICES

Experimental Details

1.0 Properties of InSb

It is well known that InSb is an extremely brittle material which is difficult to cut to a desired shape. Polycrystalline InSb, under strain or stress, has a tendency to break or shatter along the various grain boundaries. Special cutting methods have been developed by this laboratory for obtaining desired geometrical configurations from InSb ingots.

In addition to its brittleness, no little difficulty is encountered in applying good low-resistance electrical contacts to InSb specimens. Special soldering techniques have also been developed for applying contacts to the samples.

2.0 Specimen Preparation

The methods below represent a considerable saving in time and money in obtaining samples in a wide variety of configurations.

2.1 Motorized Abrasive Saw

A motor driven, self-sustaining, abrasive saw was designed and constructed for the purpose of cutting thin slices from a large ingot of InSb. The slices obtained from the ingot have a cross-section of 1" x 3/4". The thickness of the specimen may be varied anywhere in the range 1/16" to 1". A maximum crosssection of 2" x 2" can be cut by this saw.

The saw uses a mixture of water and fine mesh silicon carbide as an abrasive slurry. The specimen moves back and

forth in this slurry with the cut made by a stationary diamond impregnated bronze blade.

2.2 Hand Abrasive Saw

In addition to the motorized saw, a hand saw is used for cutting rectangles and other 'straight-line' samples from fairly thin slices of InSb. A 2" cut can be made on slices up to 1/4" in thickness.

The hand saw has a diamond impregnated bronze blade and uses a water-silicon carbide abrasive slurry.

2.3 Air Abrasive Unit

An S. S. White Industrial 'Airbrasive' Unit is used in conjunction with a turntable to cut circular disks from InSb slices. It can be used with a longitudinally moving platform to make straight line cuts.

The unit uses compressed air to supply a fine jet of abrasive material to the sample. This abrasive jet literally wears away the material to which it is applied. It is a rapid cutting tool, but can be used effectively only on slices of 3/16" or less in thickness.

2.4 Ultrasonic Drill

In addition to the cutting tools described above, a Mullard Ultrasonic drill is available for general purpose use.

3.0 Electrical Contact Application

Prior to placing the electrical contacts on the InSb specimen, it is hand lapped to the required shape and polished if desired. Then the specimen is washed in detergent and

rinsed in acetone with a final rinse in distilled water.

The electrical contacts are made by using an ultrasonic soldering iron to apply pure indium to the contact area. Since pure indium is soft and malleable, it has been found advisable to wet the contact area with a thin layer of indium and then to use a InPbSn solder for the bulk contact. This procedure results in a more stable low-resistance electrical contact.

Another method of contact application which has proved useful for low-temperature work is to vacuum deposit silver on the contact area. Then, a hard solder such as PbSn or silver solder can be used for the bulk contact.

4.0 Experimental Procedures

The schematic of the general circuit used in measuring the magnetoresistances of the various InSb specimens is shown in Figure 3-1.

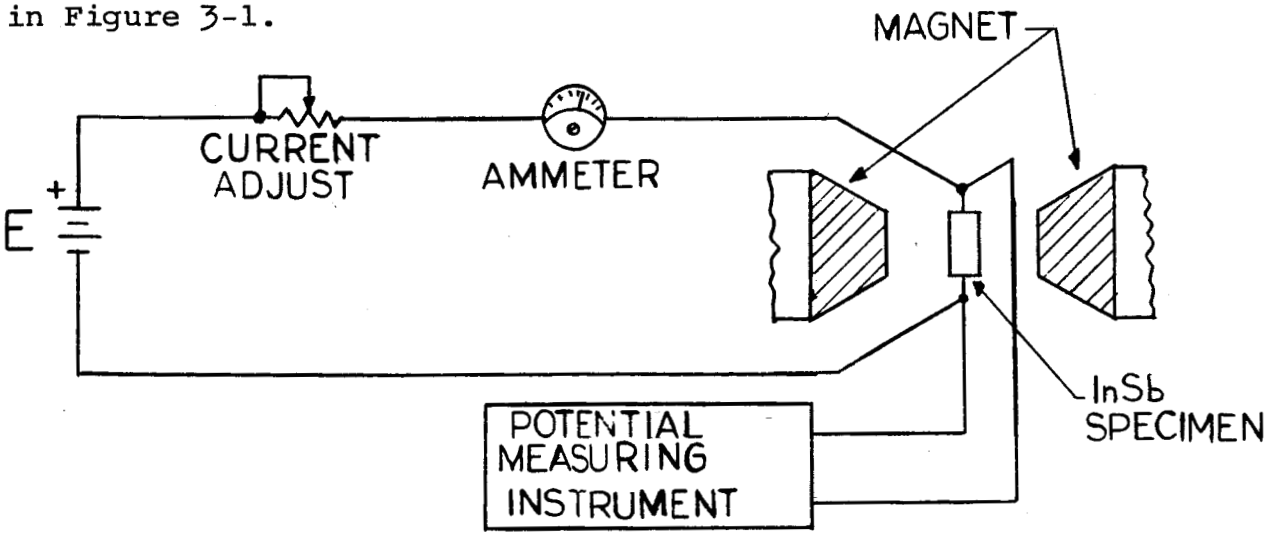

Figure 3-1. Test Circuit Schematic

The voltage source E is a 12 volt battery for low current measurements up to 15 amps. Three 6 volt batteries are connected in parallel to provide a source capable of supplying 200 amperes for five minutes into a 10 milliohm load.

The current is adjusted to the desired value by placing the proper resistance in series with the sample. The current is read on a calibrated ammeter to an accuracy of 1%.

The magnetic field is produced by a Varian electromagnet with 2" tapered pole pieces. This magnet can produce a field of 0-25 kilogauss, and has a means of reversing the direction of the field. The magnitude of the magnetic field is calibrated with a Western Electric gaussmeter having a 0.5% accuracy.

The potential measuring instrument is either a Leeds and Northrup K-2 Potentiometer or a Millivac Micro-Volt-Ammeter. The former instrument has high accuracy and resolution but is time consuming in operation. The latter instrument is fast and easy to use; however, its accuracy is on the order of 1%.

It should be pointed out that the leads for measuring the voltage drop across the specimen must be attached directly to the specimen's contacts; otherwise, a significant error is possible due to lead resistance.

All of the experimental data was obtained at either room temperature ($300^{o}k$) or at liquid nitrogen temperature($80^{o}k$). Some of the measurements were made at room temperature with the specimen maintained at this temperature by forced air

cooling. The liquid nitrogen measurements were made by placing the specimen in a test tube full of liquid nitrogen. The test tube was inserted in a styrofoam insulated container which was placed between the pole pieces of the electromagnet. The electrical leads to the specimen were inserted through holes in the rubber stopper in the test tube. By this method, the specimen could be held at 80°k for ten minutes or longer.

Experimental Results

5.0 Rectangular Slabs

5.1 Specimen #1: Figure 3-2.

Mobility, $\mu = 35{,}000$ cm^2/volt-sec

Resistivity, $\rho = 0.024$ ohm-cm

Temperature, $T = 300^{\circ}$K

Dimensions: 17/64" long
9/64" wide
4/64" thick

Sample test current = 1.0 ampere

Zero-field resistance, $R_o = 0.030$ ohm

Maximum resistance, R = 0.240 ohm at 21 Kilogauss

Percentage change in resistance per Kilogauss, n = 33.3%

Ratio of Maximum resistance to R_o, K = 8:1

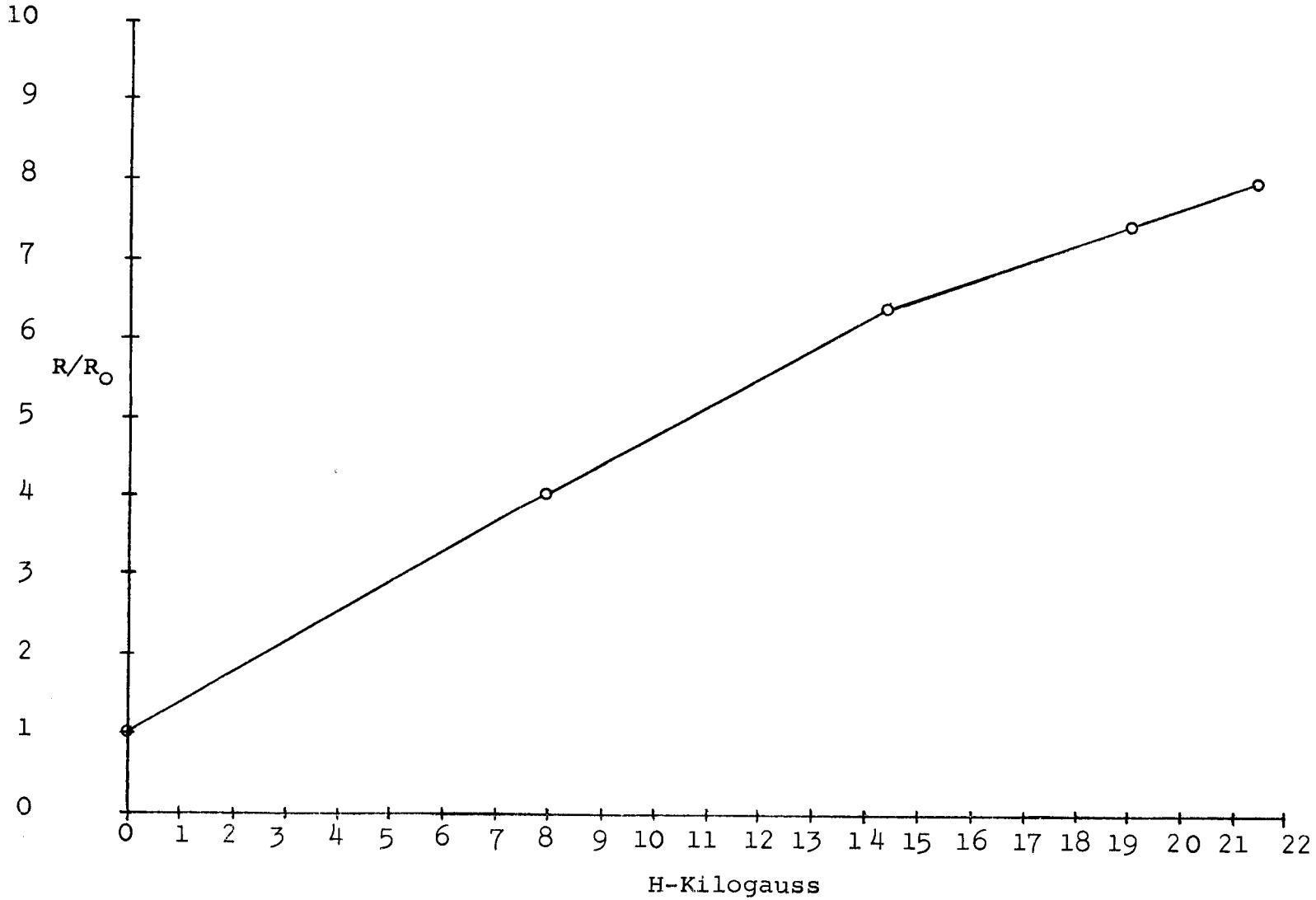

Figure 3-2
Rectangular Specimen #1

5.2 Specimen #2: Figure 3-3.

Mobility,	μ = 35,00 cm^2/volt sec
Resistivity,	ρ = 0.024 ohm-cm
Temperature,	T = 300°K
Deminsions:	17/64" long 9/64" wide 2/64" thick
Sample Test Current	= 1.0 ampere
Zero-filled resistance,	R_o = 0.067 ohm
Maximum resistance,	R = 0.400 ohm at 21 Kilogauss
Percentage change in resistance per Kilogauss,	n = 15.6%
Ratio of maximum resistance to R_o,	k = 6

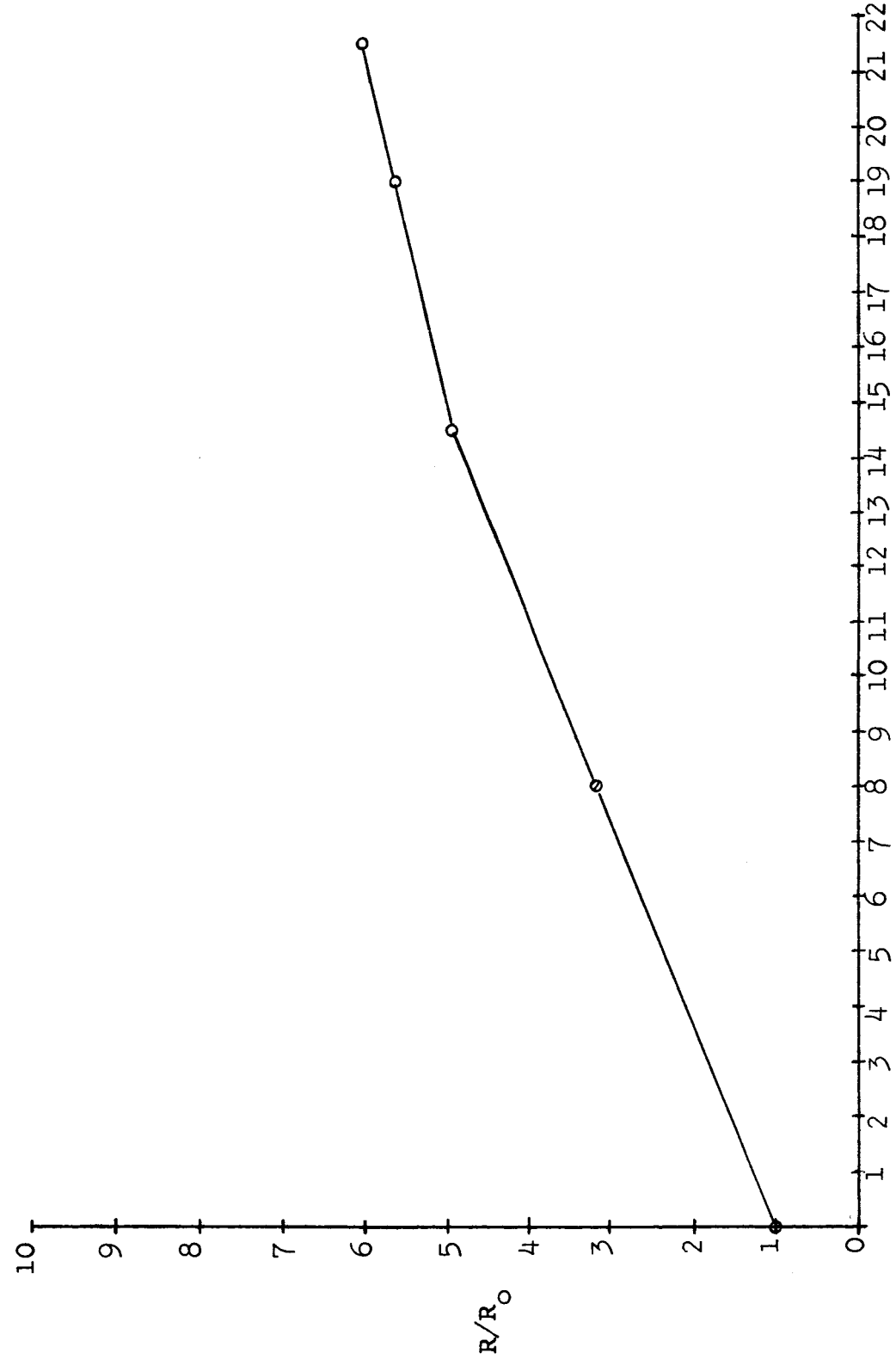

Figure 3-3 Rectangular Speciman #2

5.3 Specimen #3: Figure 3-4

Mobility, $\mu = 50{,}000\ cm^2/volt\text{-}sec$

Resistivity, $\rho = 0.006$ ohm-cm

Temperature, $T = 300^{\circ}K$

Dimensions: 1.1 cm long
0.5 cm wide
0.4 cm thick

Sample Test Current = 1.0 ampere

This particular specimen was modified by applying increasing amounts of indium along one edge and across the face to the other edge of the specimen. The magnetoresistances was measured for the various degrees of modification listed below.

5.31 Test A (Unmodified)

R_o = 0.035 ohm

R_{max} = 0.215 ohm

n = 24%

K = 6.15 : 1

5.32 Test B

R_o = 0.034 ohm

R_{max} = 0.274 ohm at 21.5 Kilogauss

n = 33%

K = 8.05 : 1

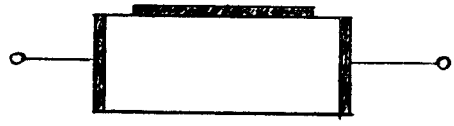

5.33 Test C

R_o = 0.029 ohm

R_{max} = 0.330 ohm

n = 48.2%

K = 11.4 : 1

5.34 **Test D**

R_o = 0.025 ohm

R_{max} = 0.332 ohm

n = 57.1%

K = 13.3

5.35 **Test E**

R_o = 0.024 ohm

R_{max} = 0.346 ohm

n = 62.4%

K = 14.4

5.36 **Test F**

R_o = 0.016 ohm

R_{max} = 0.360 ohm

n = 100%

K = 22.5

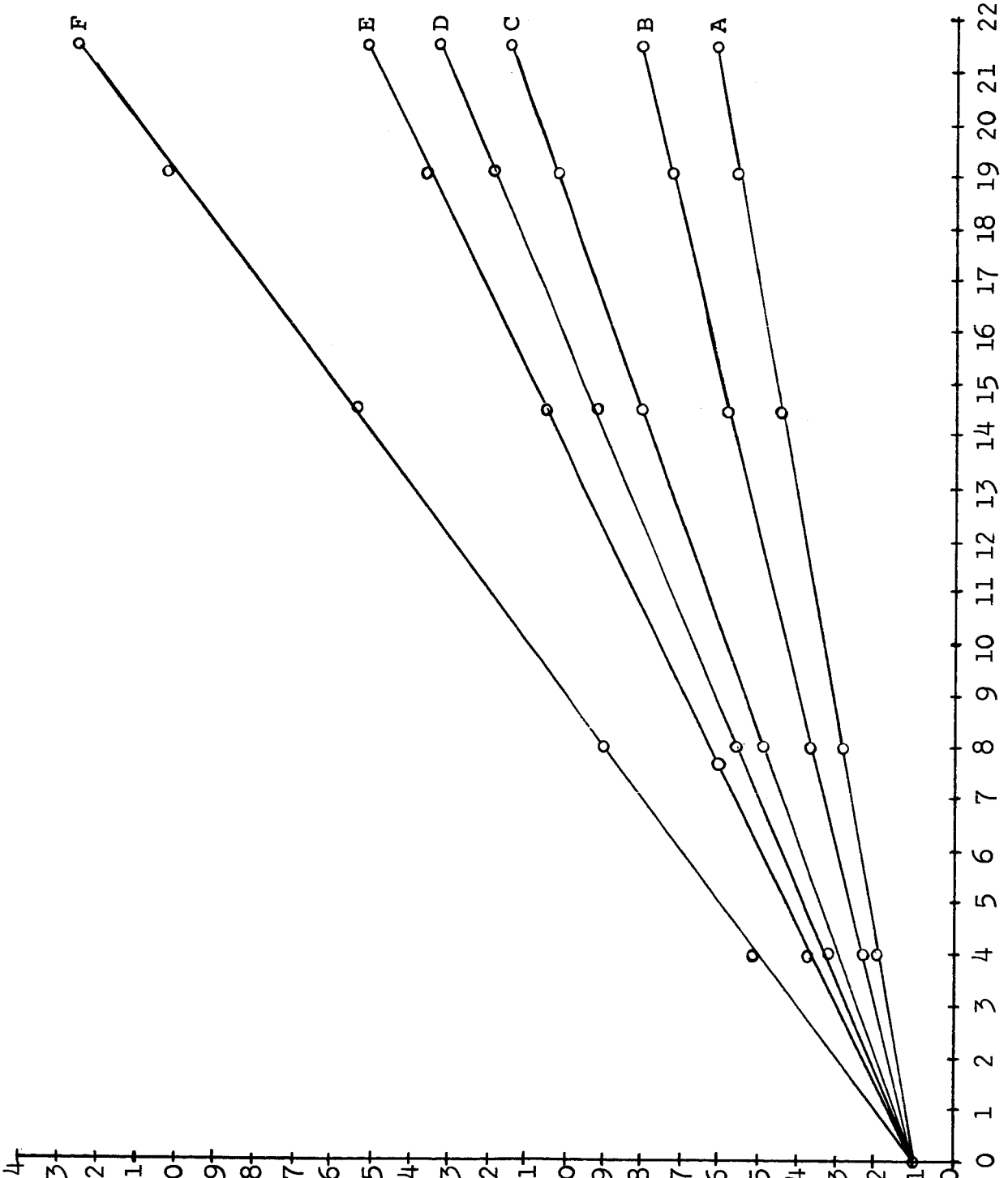

Figure 3-4. Rectangular Specimen #3

5.4 Specimen #4: Figure 3.5

Mobility, μ = 50,000 cm^2/volt-sec (300°K)

Resistivity, ρ = 0.006 ohm-cm (300°K)

Dimensions: 1.2 cm long
0.4 cm wide
0.4 cm thick

Sample Test Current = 1.0 ampere

5.41 Test #1: T = 300°K

R_o = 0.028 ohm

R_{max} = 0.102 ohm at 10 Kilogauss

n = 26.4%

K = 3.64

5.42 Test #2: T = 80°K

R_o = 0.850 ohm

R_{max} = 7.1 ohm at 10 Kilogauss

n = 73.5%

K = 8.35

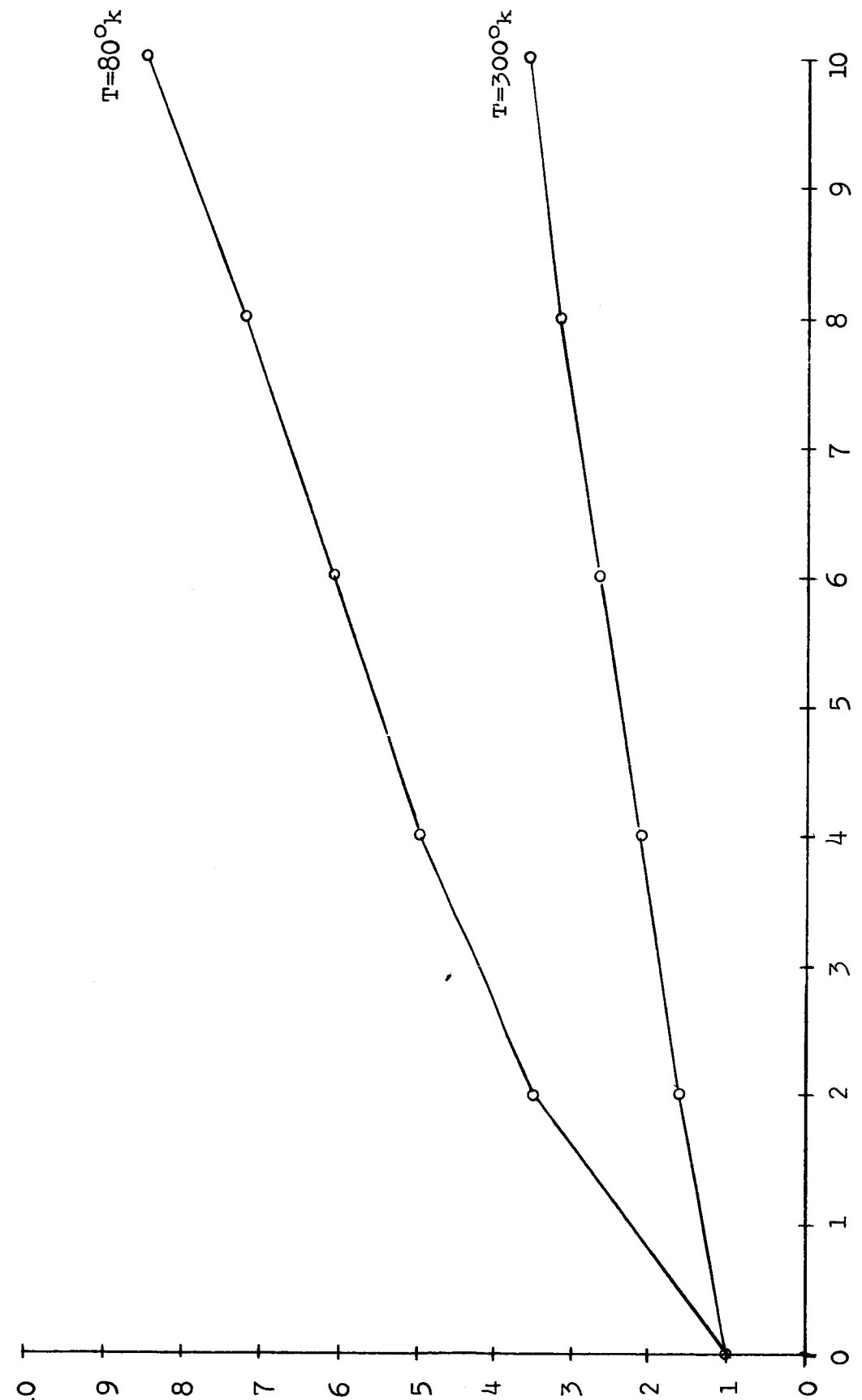

Figure 3-5. Rectangular Specimen #4

6.0 Corbino Disks

6.1 Specimen #1: Figure 3.6

Mobility,	μ = 50,000 cm^2/volt-sec
Resistivity,	ρ = 0.006 ohm-cm
Temperature,	T = 300°K
Dimensions:	0.96 cm outer radius 0.13 cm inner radius 0.32 cm thickness
Sample Test Current	= 1.0 ampere
Zero-field resistance,	R_o = 0.006 ohm
Maximum resistance,	R = 0.163 ohm at 21.5 Kilogauss
Percentage change in resistance per Kilogauss,	n = 73%
Ratio of maximum resistance to R_o,	K = 27.2

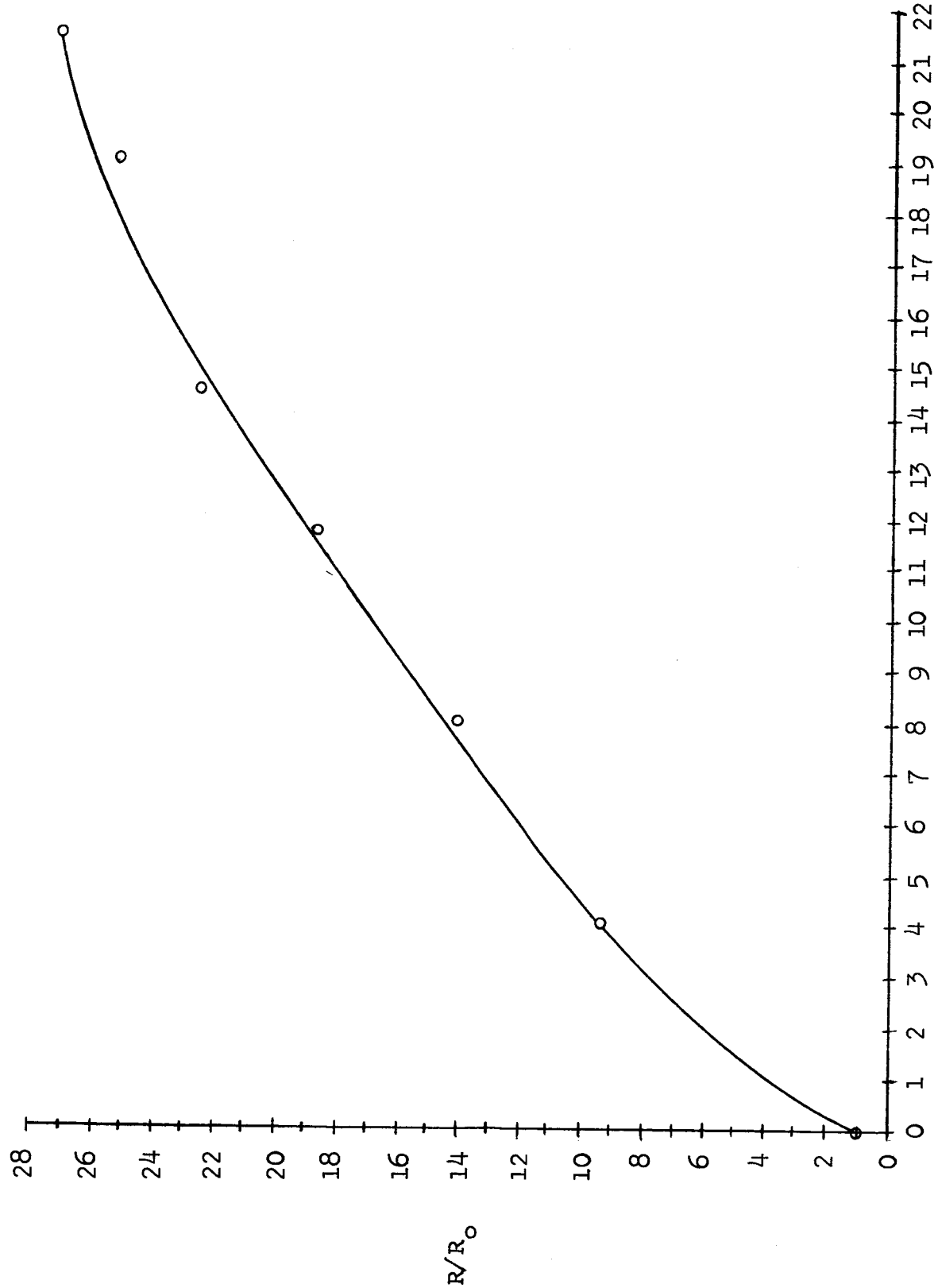

Figure 3-6. Corbino Disk, Specimen #1

6.2 Specimen #2: Figure 3-7

Mobility,	μ = 65,000 cm^2/volt-sec
Resistivity,	ρ = 0.005 ohm-cm
Temperature,	T = 300°K
Dimensions:	0.9 cm outer radius 0.24 cm inner radius 0.32 cm thickness
Sample Test Current	= 1.0 ampere
Zero-field resistance,	R_o = 0.0041 ohm
Maximum resistance,	R = 0.210 ohm at 20 Kilogauss
Percentage change in resistance per Kilogauss,	n = 251%
Ratio of maximum resistance to R_o,	K = 51.2

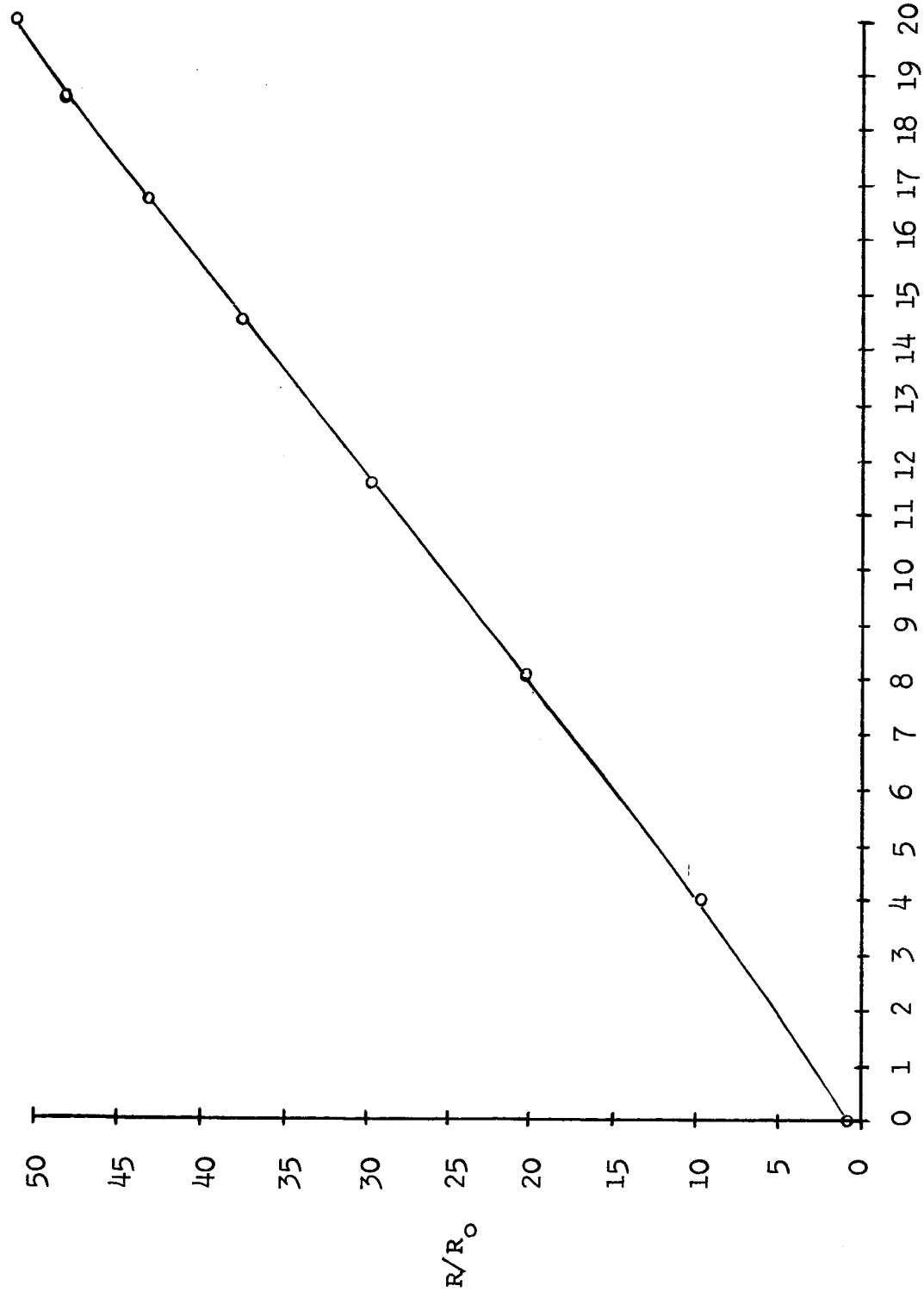

Figure 3-7. Corbino Disk, Specimen #2

6.3 Specimen #3: Figure 3-8

Mobility,	μ = 65,000 cm^2/volt-sec
Resistivity,	ρ = 0.005 ohm-cm
Temperature,	T = 300°K
Dimensions:	0.9 cm outer radius 0.24 cm inner radius 0.32 cm thickness
Sample Test Current	= 1.0 ampere
Zero-field resistance,	R_o = 0.012 ohms
Maximum resistance,	R = 0.180 ohms at 10 Kilogauss
Percentage change in resistance per Kilogauss,	n = 150%
Ratio of maximum resistance to R_o,	K = 15

This specimen was later measured at liquid nitrogen temperature (80°K) with the following results:

Temperature,	T = 80°K
Sample Test Current,	= 1.0 ampere
Zero-field resistance,	R_o = 0.075 ohm
Maximum resistance,	R = 3.94 ohm at 10 Kilogauss
Percentage change in resistance per Kilogauss,	n = 515%
Ratio of maximum resistance to R_o,	K = 52.5

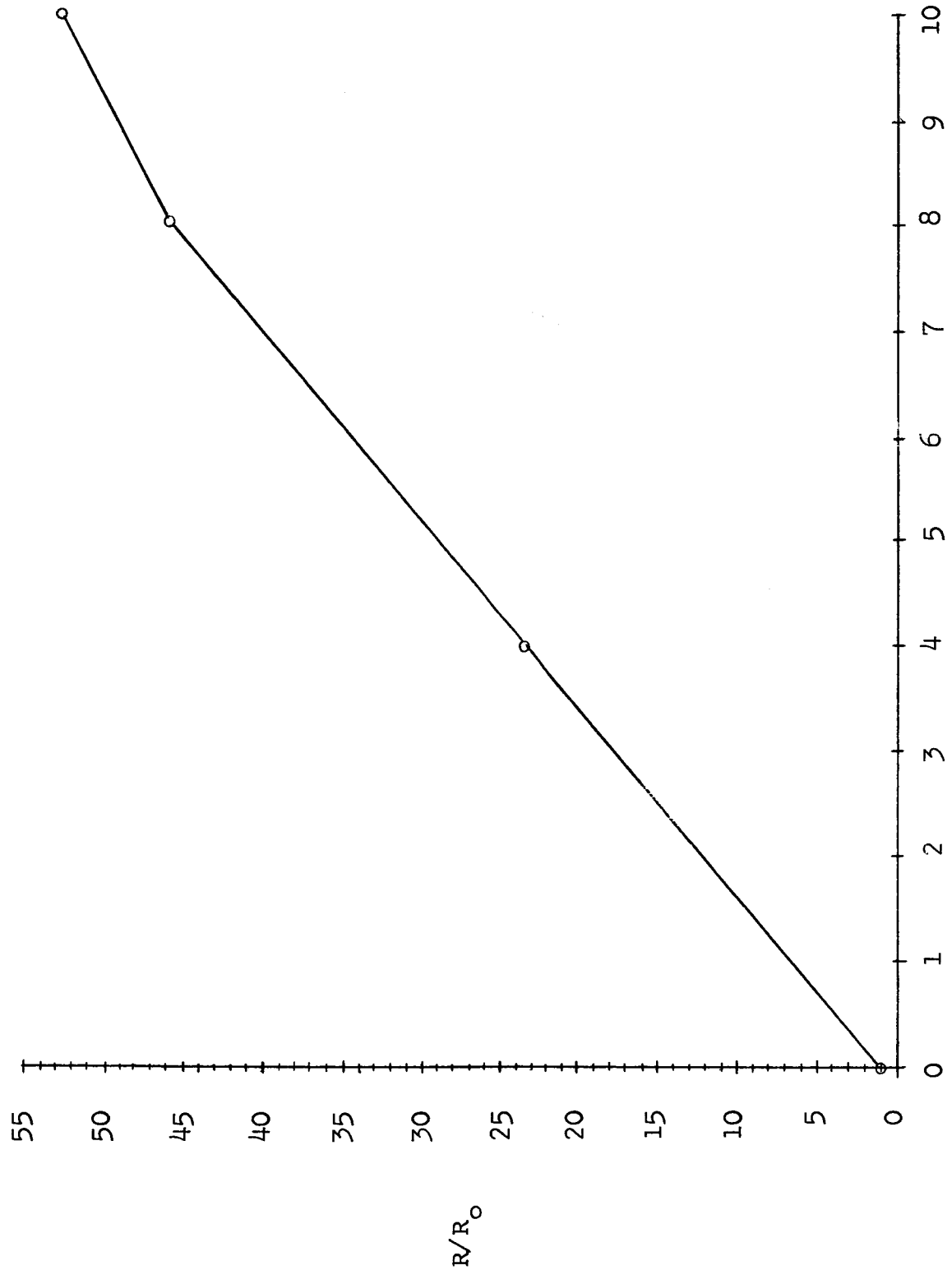

Figure 3-8. Corbino Disk #3

7.0 Miscellaneous Geometrical Configuration

7.1 Specimen #1: Figure 3-9

Geometry:

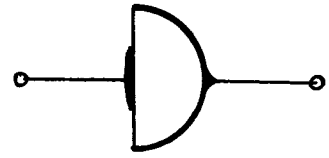

Mobility,	μ = 65,000 cm^2/volt-sec
Resistivity,	ρ = 0.005 ohm-cm
Temperature,	T = 300°K
Dimensions:	1/2 disk of 1.0 cm radius
Sample Test Current	= 1.0 ampere
Zero-field resistance,	R_o = 0.007 ohm
Maximum resistance,	R = 0.196 ohm at 20 Kilogauss
Percentage change in resistance per Kilogauss,	n = 140%
Ratio of maximum resistance to R_o,	K = 28

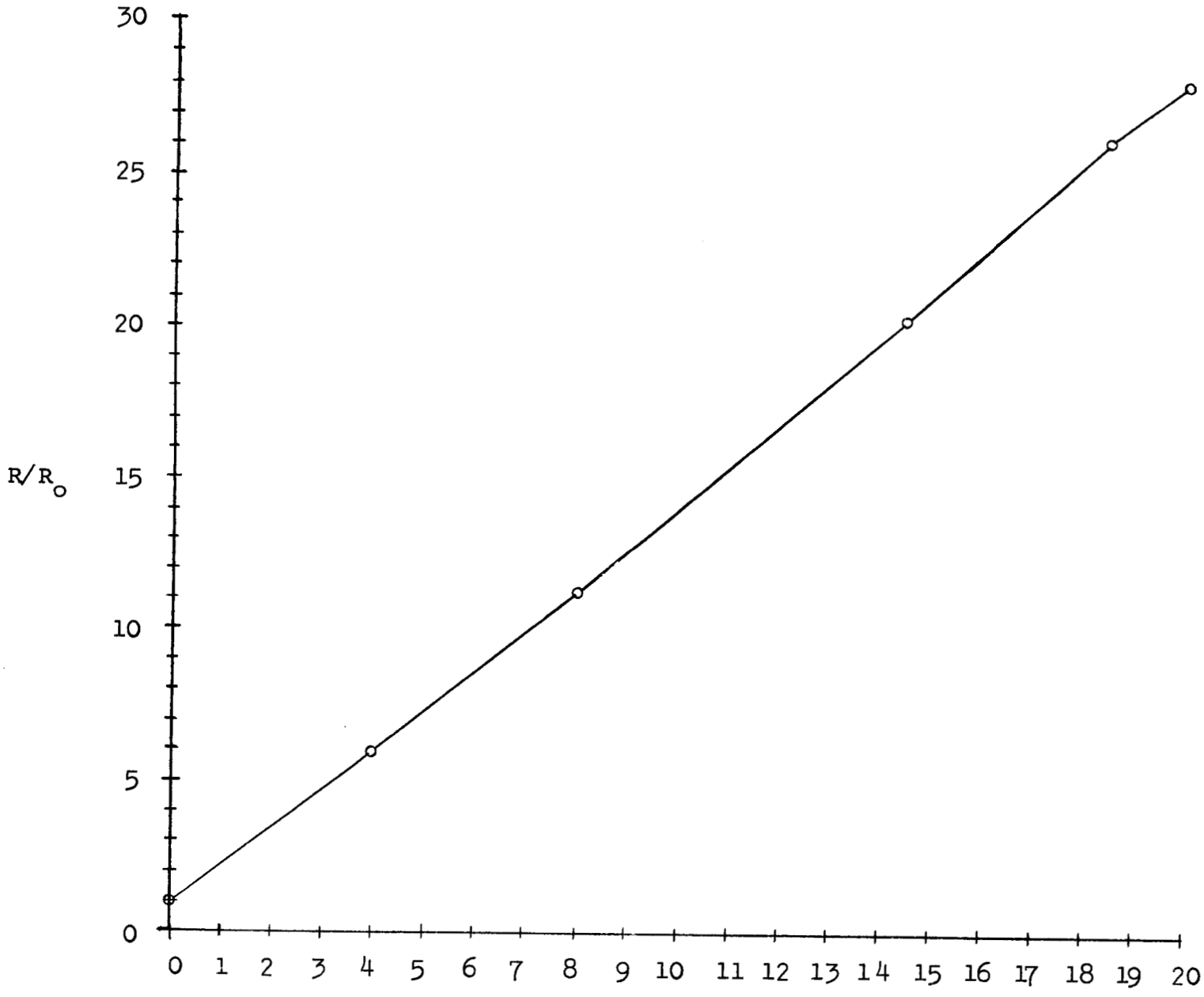

Figure 3-9. Miscellaneous Specimen #1

7.2 Specimen #2: Figure 3-10

Geometry:

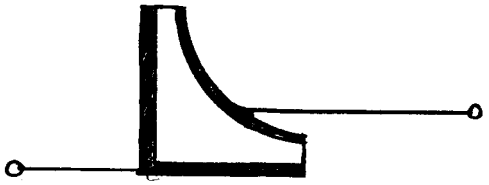

Mobility,	μ = 65,000 cm^2/volt-sec
Resistivity,	ρ = 0.005 ohm-cm
Temperature,	T = 300°K
Dimensions:	r = 0.9 cm l = 1.0 cm t = 0.2 cm
Sample Test Current	= 1.0 ampere
Zero-field resistance,	R_o = 0.0035 ohm
Maximum resistance,	R = 0.175 ohm at 21.5 Kilogauss
Percentage change in resistance per Kilogauss,	n = 232%
Ratio of maximum resistance to R_o,	K = 50

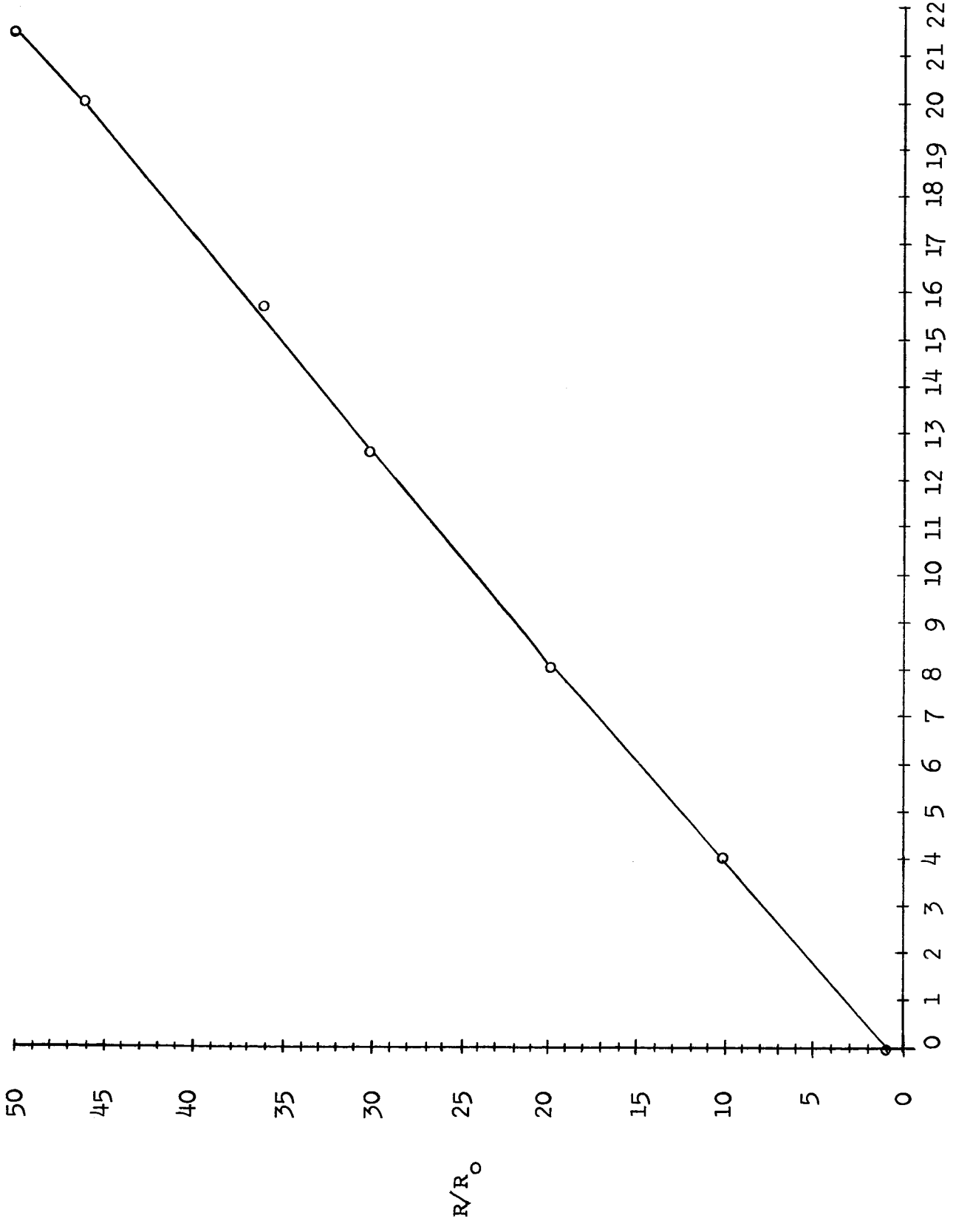

Figure 3-10. Miscellaneous Specimen #2

7.3 Specimen #3: Figure 3-11

Geometry: Duo-Magnetoresistor

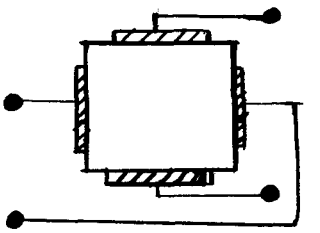

Dimensions: 3/4" long
3/4" wide
1/8" thick

Mobility, $\mu = 65{,}000\ cm^2/volt\text{-}sec$

Resistivity, $\rho = 0.005$ ohm-cm

Temperature, $T = 300^{\circ}K$

Zero field resistance, $R_{01} = V_1/I_1 = 0.029$ ohm
$R_{02} = V_2/I_2 = 0.030$ ohm

Sample Test Currents $I_1 = I_2 = 1.0$ ampere

Resistances at 20 Kilogauss with field normal, $R_1 = V_1/I_1 = 0.038$ ohm
$R_2 = V_2/I_2 = 0.380$ ohm

Resistances at 20 Kilogauss with field reversed, $R_1 = V_1/I_1 = 0.360$ ohm
$R_2 = V_2/I_2 = 0.046$ ohm

From the graph of Figure 3-11:

$$\frac{R_{1max}}{R_{1min}} = 19.5$$

$$\frac{R_{2max}}{R_{2min}} = 16.9$$

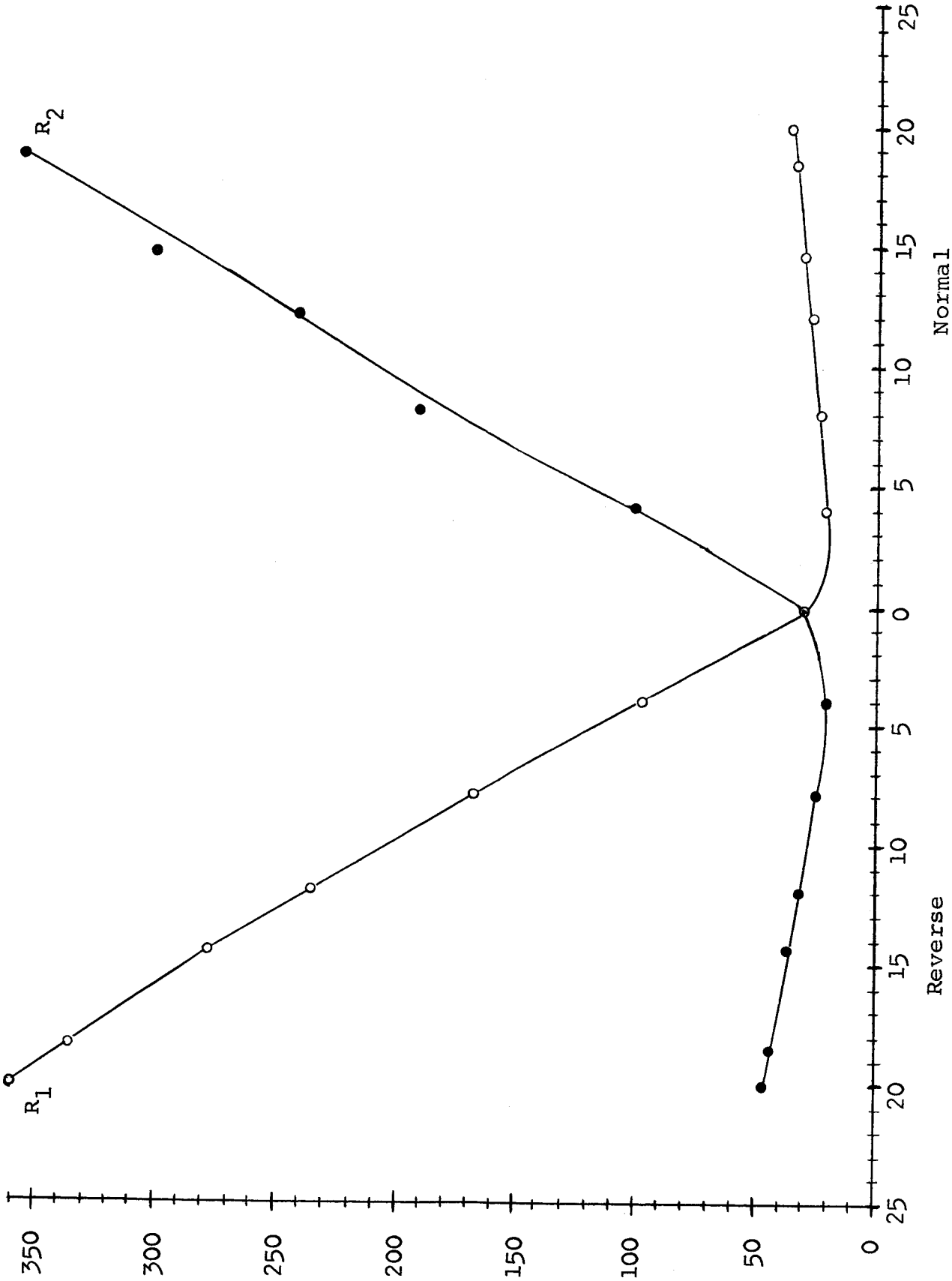

Figure 3-11. Miscellaneous Specimen #3

7.4 Specimen #4: Figure 3-12

This specimen is physically the same as specimen #3, the duo-magnetoresistor. In this series of measurements, the current I_2 is adjusted such that the input resistance seen at terminal pair #1 becomes zero for a magnetic field of 20 Kilogauss in the reverse direction.

The important test parameters are:

$T = 300^{\circ}K$

$I_1 = 1.0$ ampere

$I_2 = 1.24$ ampers

$R_{01} = 0.029$ ohm

$R_{02} = 0.030$ ohm

$R_{1max} = 0.390$ ohm at 20 Kilogauss, normal

$R_{1min} = 0.000$ ohm at 20 Kilogauss, reverse

$R_{2max} = 0.315$ ohm at 20 Kilogauss, reverse

$R_2 = 0.069$ ohm at 20 Kilogauss, normal

$R_{2min} = 0.026$ ohm at 20 Kilogauss, normal

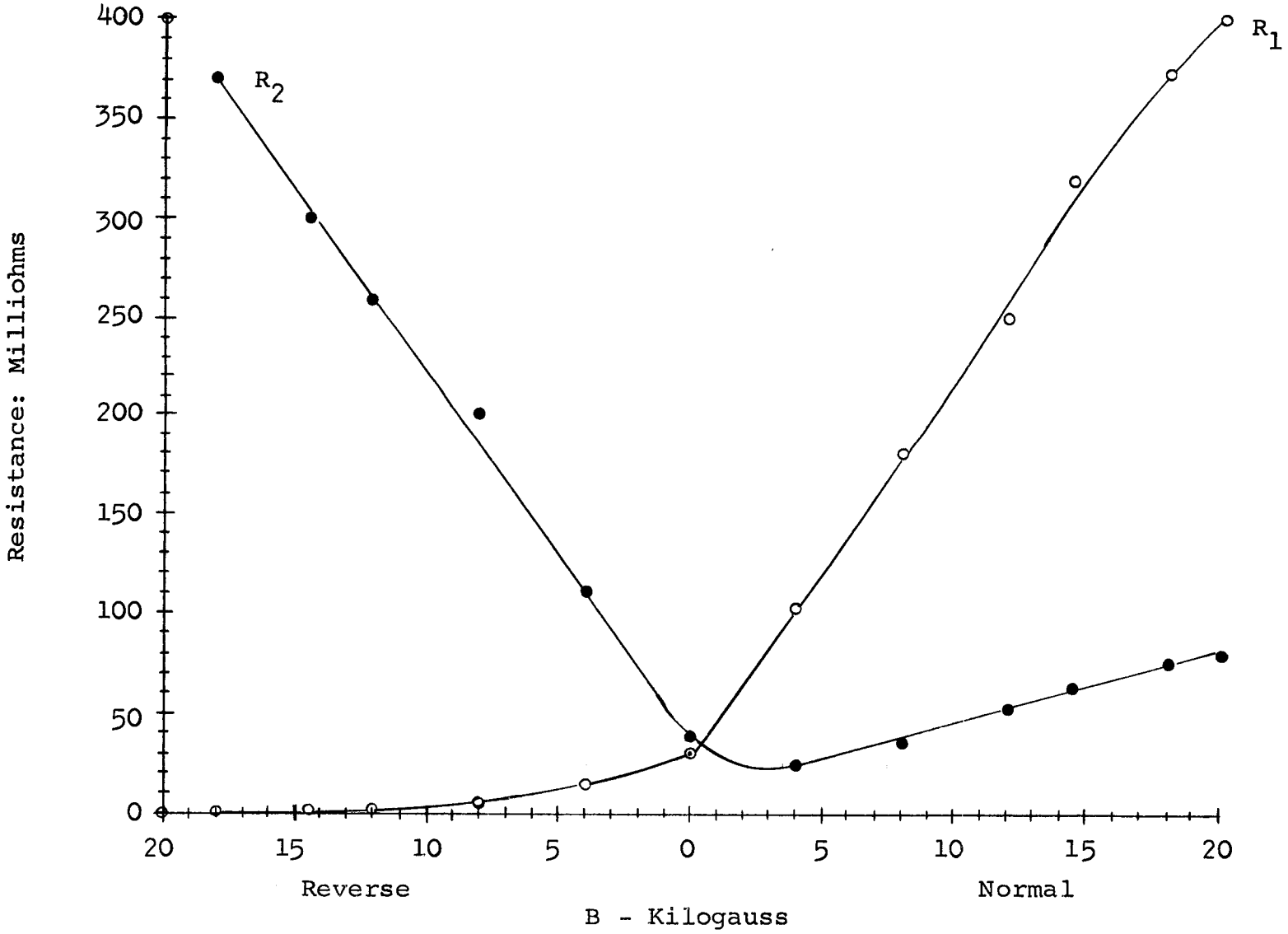

Figure 3-12. Miscellaneous Specimen #4

Conclusion

This chapter describes the special equipment and procedures involved in the preparation of InSb magnetoresistance devices. The preparation of each specimen requires a great deal of time consuming and cautious effort as a result of extreme brittleness of InSb crystals. With the crystal cutting and shaping equipment available at the present time, any reasonable geometrical configuration of InSb can be manufactured without undue difficulty.

A number of measurements performed on InSb specimens having various geometries have been presented here. These experimental results are representative of the types of magnetoresistance devices which have been tested in the course of this research.

The experimental data indicate that of the more common geometries, the Corbino disk is the most useful magnetoresistance device. Other geometrical configurations have been tested, of which the duo-magnetoresistor has the most unusual characteristics. In this device, it is possible to attain a great variety of magnetoresistance effects by biasing one terminal pair and measuring the magnetoresistance at the other terminal pair.

The value of K = 51.2 has been experimentally obtained but more work is needed to improve this on field to off field resistance ratio.

CHAPTER IV. CIRCUIT ANALYSES

1.0 Background

Several circuit configurations have been studied in order to maximize the converter efficiency and flexibility using magnetoresistive devices. One of the better circuits is shown in Fig. 4.1. With this configuration only a.c. flows through the output branch in the idealized case--with a square wave magnetic input. This is important since a.c. is the only usable output for transformation and rectification, and the d.c. results in only a power loss.

In analyzing this circuit below, the transformer and circuit losses will be neglected and a square wave current form will be assumed. It will be shown that for design purposes the same equations can be used to maximize the efficiency when circuit resistance is included.

1.1 Theory

With reference to Fig. 4.1, the branch currents for the first half cycle are as follows:

$$i_{11} = \frac{E(1-K)}{KR_L+R_L+2Kr_o} \qquad (4.1)$$

$$i_{21} = \frac{E\left(\frac{R_L+r_o}{r_o}\right)}{KR_L+R_L+2Kr_p} \qquad)4.2)$$

$$i_{31} = \frac{-E\left(\frac{R_L+Kr_o}{r_o}\right)}{KR_L+R_L+2Kr_o} \qquad (4.3)$$

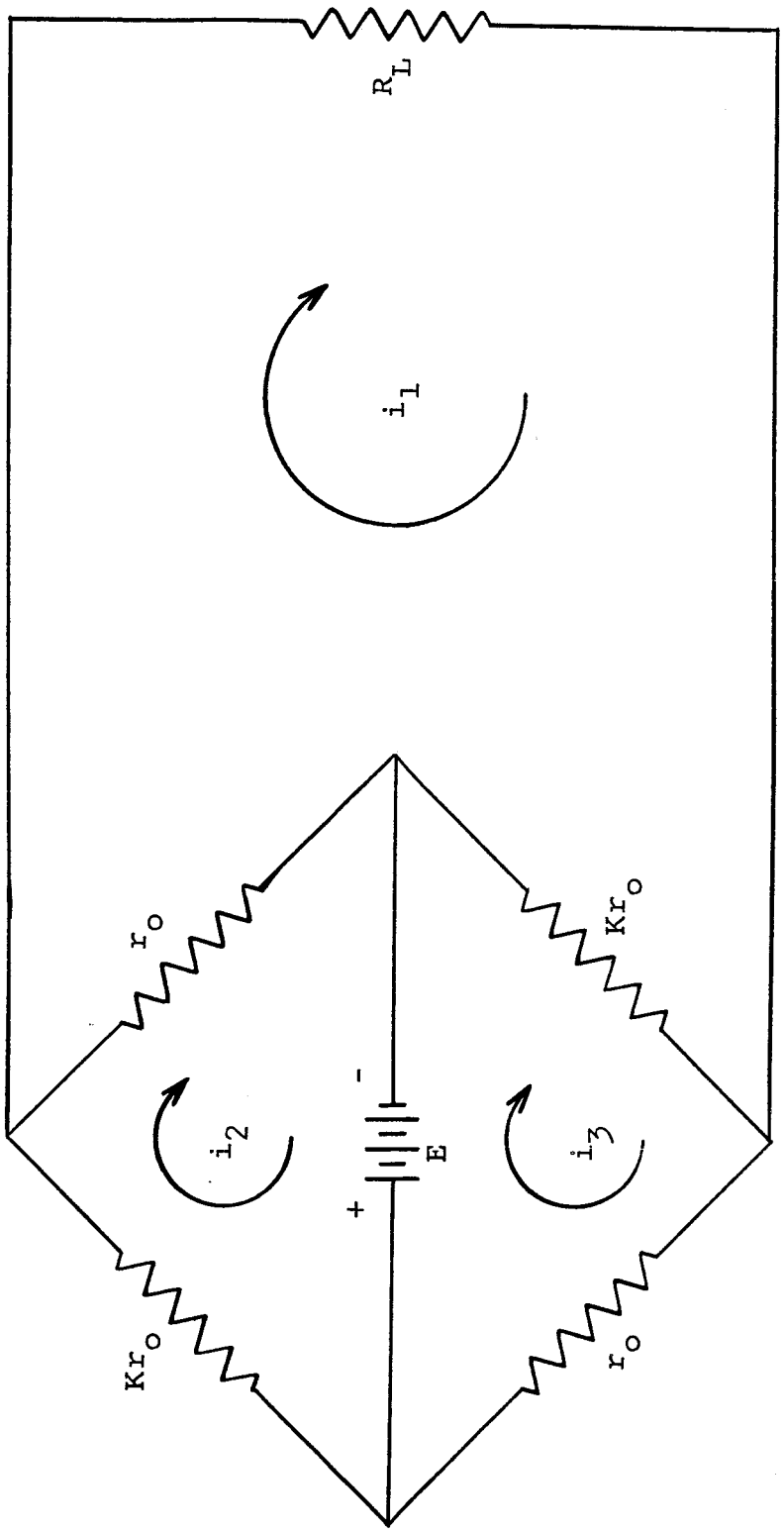

Figure 4-1. Magnetoresistance Converter Circuit

where

R_L = the a.c. output resistance

r_o = the static resistance of the magnetoresistive device

K = the magnetoresistance ratio

For the second half cycle, the current relations are

$$i_{12} = -i_{11} \tag{4.4}$$

$$i_{22} = -i_{31} \tag{4.5}$$

$$i_{32} = -i_{21} \tag{4.6}$$

As shown above, the currents are constant in direction and magnitude in the bridge, and alternating, but constant in magnitude, through the a.c. load. Therefore, the input power from the source is constant and can be written as

$$P_{in} = P_{dc} = (i_2 - i_3)E \,. \tag{4.7}$$

In the output circuit the rms current equals the a.c. so that the output power is

$$P_{ac} = i_1^2 \, R_L \,. \tag{4.8}$$

Hence, the efficiency expression becomes

$$\eta = \frac{P_{ac}}{P_{dc}} = \frac{\frac{R_L}{r_o}(1-K)^2}{(\frac{R_L}{r_o})^2(2K+2)+\frac{R_L}{r_o}(K^2+6K+1)+(2K^2+2K)} \,. \tag{4.9}$$

Plots of efficiency versus R_L/r_o are shown in Fig. 4.2.

In the limiting case of a perfect switch

$$\lim_{\substack{K \to \infty \\ r_o \to 0}} \eta = \frac{R_L}{R_L} = 100\% \,.$$

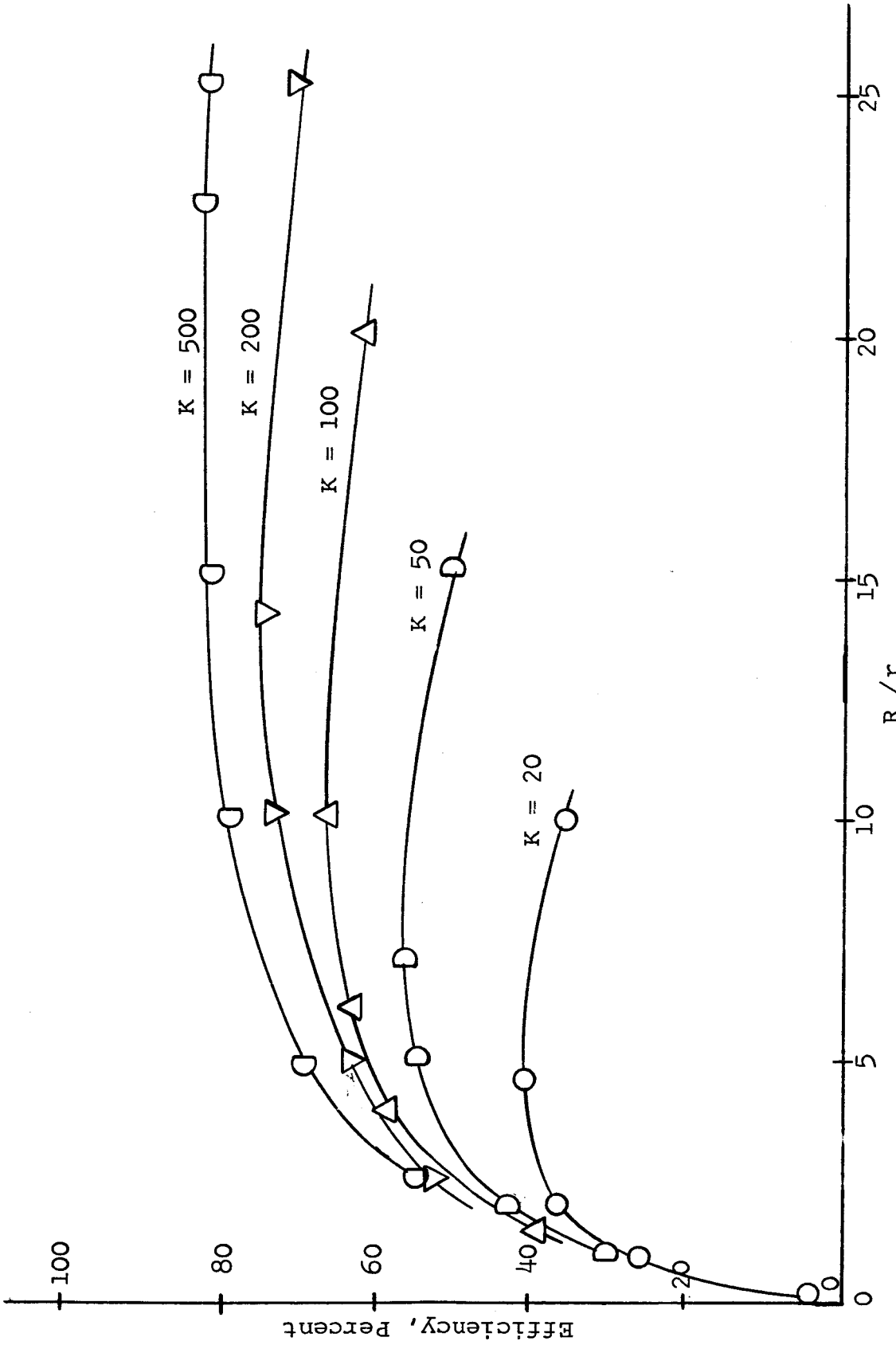

Figure 4-2. Efficiency vs R_L/r_o for Circuit of Figure 4-1.

An expression for the maximum ratio of R_L to r_o as a function of K is useful information and can be derived by letting

$$\frac{d\eta}{dR_L/r_o} = 0$$

which gives

$$\left.\frac{R_L}{r_o}\right|_{\eta\,max} = (K)^{1/2} . \qquad (4.10)$$

A plot of maximum efficiency versus K is shown in Fig. 4.3.

A magnetoresistance ratio of 51.2 at <u>room temperature</u> has been obtained experimentally by this laboratory. Using this figure, the maximum theoretical efficiency can be derived by combining equations 4.10 and 4.9.

$$\eta_{max} = \frac{K^{1/2}(1-K)^2}{K(2K+2) + K^{1/2}(K^2+6K+1)+(2K^2+2K)} \qquad (4.11)$$

for K = 51.2

$$\eta_{max} = 57.3\% .$$

1.11 For design purposes a close approximation to actual circuit conditions can be obtained as follows:

If $r_o = r_c + r_d$,

and $Kr_o = r_c + K' r_d$,

where r_c = circuit resistance,

r_d = static device resistance,

K' = magnetoresistance ratio .

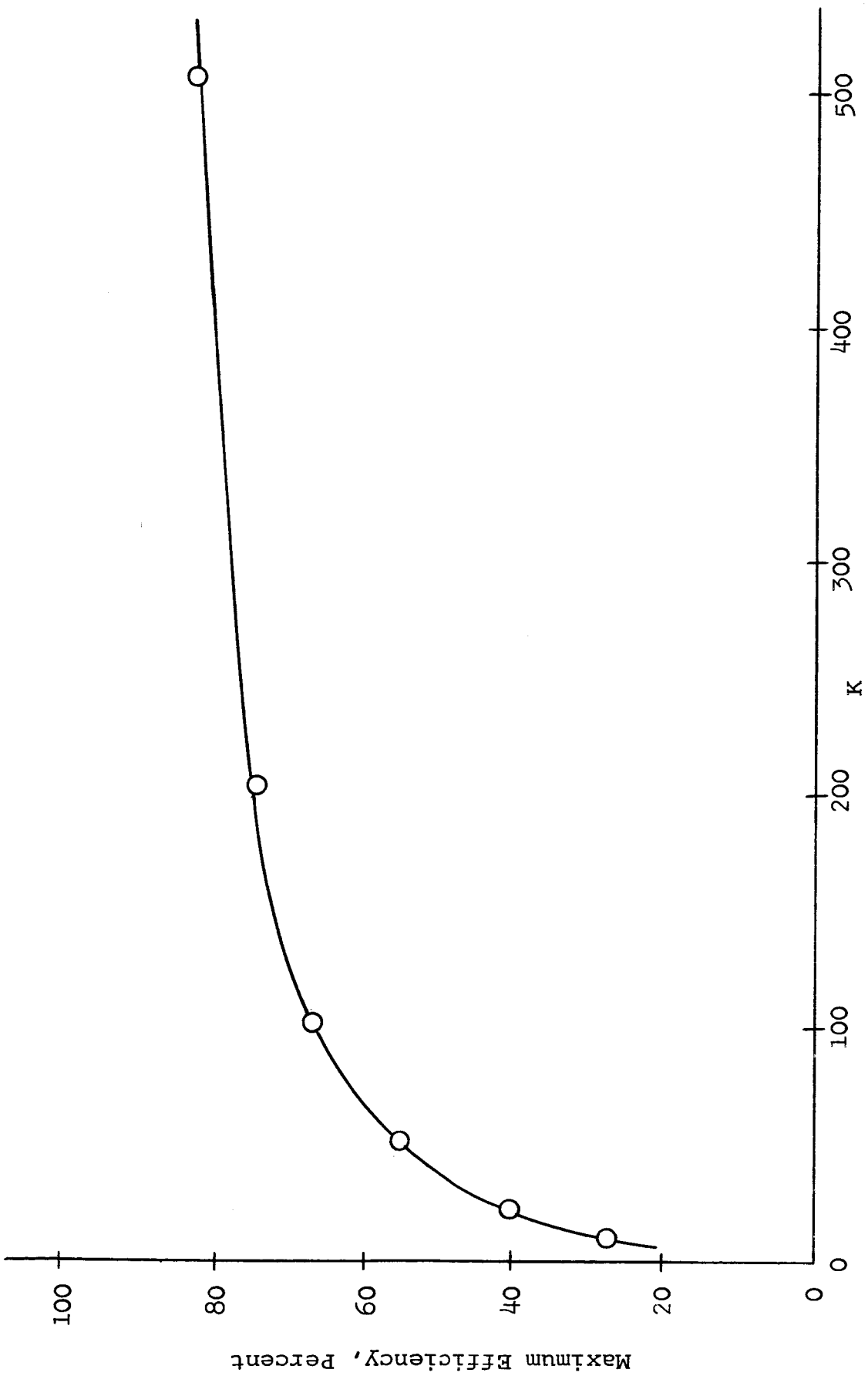

Figure 4.3. Maximum Theoretical Efficiency vs Magnetoresistance Ratio

then the following expression would provide most of the knowledge needed, including some transformer and load-matching information, to obtain a maximum efficiency for a particular K'.

$$\frac{R_{ac}}{r_c+r_d}\Bigg|_{\eta\ max}^{for} = (K)^{1/2} = \left[\frac{r_c+K'r_d}{r_c+r_d}\right]^{1/2} . \qquad (4.11)$$

2.0 Advantages of the Magnetoresistance Converter

The so-called unconventional power sources, such as thermoelectric generators, fuel cells, solar cells, etc., all have one common characteristic--high-current, low-voltage operation. Typically these power sources operate in the range of a fraction of a volt to 1.5 volts. Any attempt to connect them in series to increase the output voltages tends to lower the reliability and the economy of operation of such sources.

The best approach is to use one fraction-volt high-current source and switch the current into a step-up transformer. The a.c. output can then be rectified to the d.c. voltage-current balance desired.

Unfortunately, transistors, tunnel diodes, and other solid-state switching devices capable of handling extremely high currents at fractions of a volt efficiently are virtually non-existent today. Currently transistors appear to be the best of the active devices, however the highest power transistor available, the 100 ampere Pacific epitaxial planar transistor, has a saturation resistance in the 0.01 to 0.04

range, making it extremely inefficient at less than two volts input with a source current of 100 amperes.

Several d.c.-a.c. converter circuits using transistors have been studied by Electro-Optical Systems, Inc.* They found the best circuit to be the Dreisbach converter. Using 32 MHT 1903 power transistors (16 paralleled, perfectly and completely matched transistors per unit), this converter was found to have a theoretical efficiency (neglecting transformer and circuit losses) of 43% at 0.5 volts and 100 amperes. Compare this to the theoretical efficiency of 57.3% (for the experimentally obtainable K of 51.2) for the magnetoresistance converter shown in Figure 4.1, and the potential efficiencies obtainable for higher values of K as described in Figure 4.3. Too, it is important to realize that the efficiency of this magnetoresistance converter is independent of source voltage.

*"Low Input Converter Study," Progress Report, Electro-Optical Systems, Inc., August 1962

CONCLUSION

The classical theory of magnetoresistance derived from the free electron model does not fit high purity indium antimonide, because the density of the energy levels and the scattering mechanisms are functions of the magnetic field. Magnetoresistance effects predicted by the quantum theory vary from quadratic dependence on magnetic field for very low fields to a linear dependence on magnetic field for a very high field. In the case of indium antimonide, the magnetoresistance is essentially a linear function of the magnetic field. Geometry of the specimen has a large effect upon its magnetoresistance. The maximum magnetoresistance should occur when the effect of the Hall field is minimized. The Corbino disk is a good configuration for this purpose.

An on-field to off-field resistance ratio, K, of 51.2 has been experimentally obtained at room temperature. For this ratio a conversion efficiency of 57.3% is predicted for the circuit configuration shown in Figure 4.1. The efficiency is, of course, highly dependent on the on-field to off-field ratio as has been shown by figure 4.3. More work is needed to increase the value of this ratio at room temperatures. Using liquid nitrogen as a coolant it is possible to increase the value of K (experimental results) by a factor of approximately 4. Theoretically the increase should be even larger, especially for higher purity material. If one assumes a value of 200 for K, the theorical conversion efficiency goes up to 75.3%

Most of the experimental measurements have been made for a current of about 1 ampere. This was done as a matter of convenience for the initial experiments, as it should be possible to construct a device capable of carrying on the order of 100 amperes or more. The efficiency of the converter should not be affected by the amount of current or the source voltage (assuming the temperature is held to the same value as in the low current case). It is not difficult to fabricate InSb devices with off-field impedances of .001 ohms or less. If bismuth can be used, even lower impedances are possible.

FUTURE WORK

1. A comprehensive theoretical study of the dependence of magnetoresistance on sample geometry, physical properties and temperature will be continued in conjunction with similar experimental studies. The primary goal of these studies is to maximize the on-field to off-field resistance for indium antimonide specimens.

2. Some of the magnetoresistance properties of bismuth will be investigated. Bismuth has an extremely low impedance which is a desirable property for high current devices and has some very interesting magnetoresistance properties, especially at low temperatures.

3. A study will be made on combining the Hall effect with magnetoresistance to determine if the combination devices can be made better than a strictly magnetoresistance device.

4. A feasibility study will be made on Hall devices using smooth or rough surfaces and possibly the use of interface surfaces to improve the on-field to off-field ratio.

5. The circuit study will continue theoretically and with some preliminary experiments.